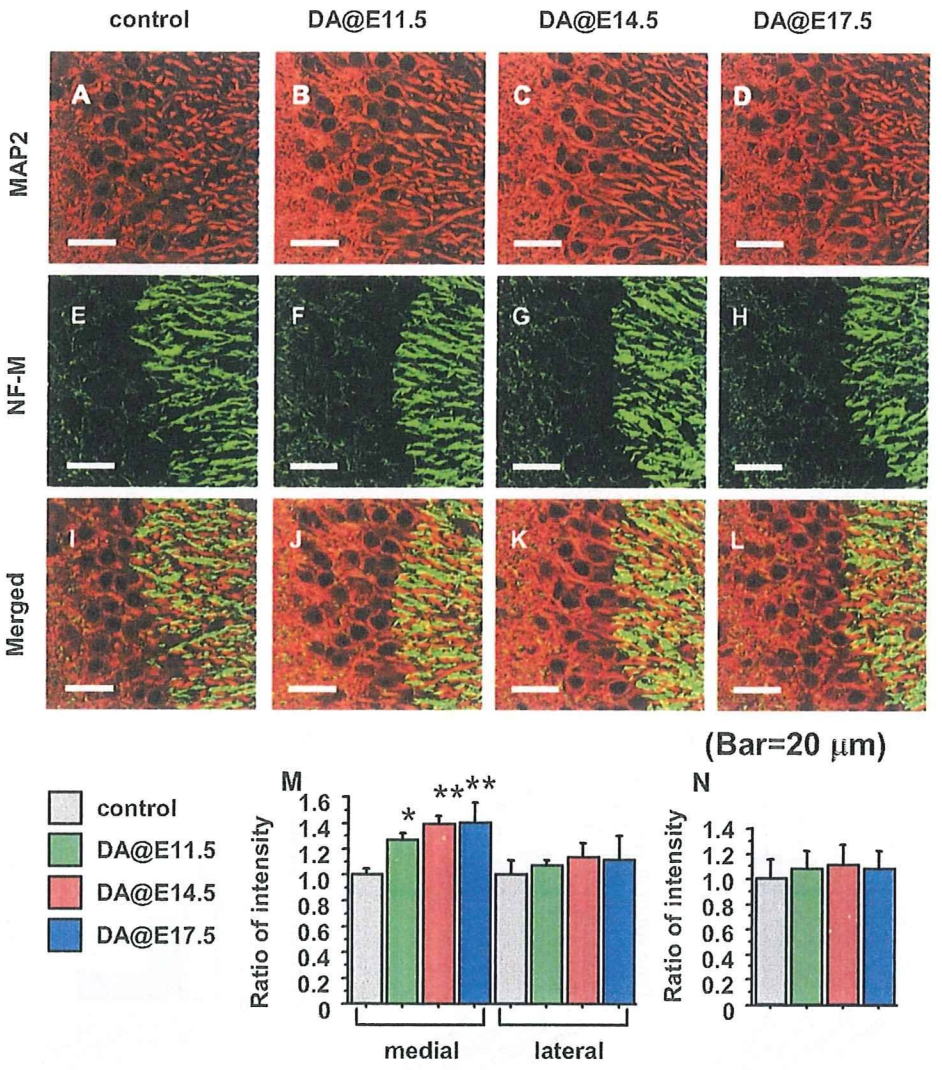

Fig. 2. Delayed effects on hippocampus induced by prenatal exposure of DA.
A-D, Immunohistochemical staining against MAP2; E-H, immunohistochamical staining against NF-M; I-L, merged images, of CA3 hippocampus. A, E, I, group A (control), B, F, J, group B (DA@11.5), C, G, K, group C (DA@14.5) and D, H, L, group D (DA@17.5). Scale bar = 200 mm. M, Quantitative analysis of MAP2 expression, and N, NF-M expression among the groups (mean ± S.E.M.). Asterisk (**) and (*) indicated significant difference compared to control ($P < 0.01$) and ($P < 0.05$).

ing maturation, such as hyperreactivity to handling and to cage mates, and did not present overt malformation of the brain detectable by the routine H&E histology at the age of 2 weeks (data not shown). It is also noted that the spectrum of the neurobehavioral symptoms induced in mice exposed to DA at adulthood was different from those monitored in this study (data not shown).

Although progressive hippocampal neuronal damages were reported to be induced by prenatal administration of DA (0.6 mg/kg intravenous injection to the dam) (Dakshinamurti *et al.*, 1993), we did not find notable neuronal loss or neuronal cell death as the delayed effects in adult mouse brain by prenatal exposure. On the other hand, we found myelination failure (Miller and Mi, 2007) in cortex of group B (DA@11.5) and C (DA@14.5) mice. And we also detected a finding compatible with the overgrowth of neuronal processes in cortex and hippocampus of group B (DA@11.5), C (DA@14.5) and D (DA@14.5)

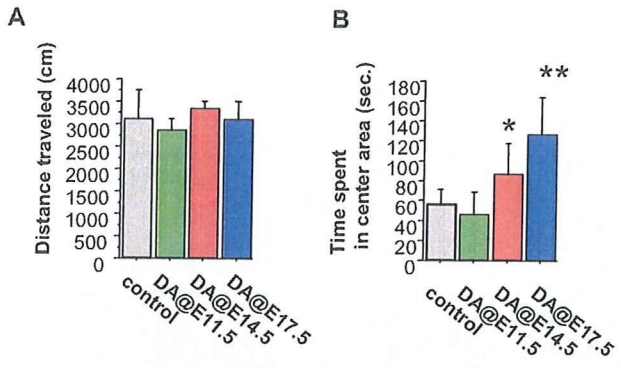

Fig. 3. Delayed effects on locomotor activity (OF test) induced by prenatal exposure of DA.
A, Mean distance travelled (total distances divided by total duration of trial, 10 min) and B, mean time spent in center area (30% of the field) in the open field apparatus (mean ± S.E.M.). Asterisk (**) and (*) indicated significant difference compared to control ($P < 0.01$) and ($P < 0.05$).

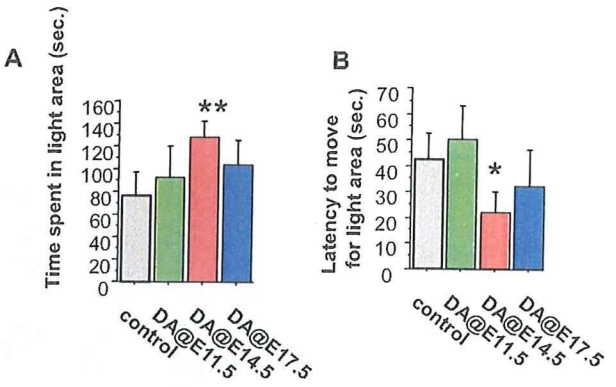

Fig. 4. Delayed effects on anxiety-related behavior (LD test) induced by prenatal exposure of DA.
A, Total time spent in light area, and B, latency time to move to light area in the LD apparatus (mean ± S.E.M.). Asterisk (**) and (*) indicated significant difference compared to control ($P < 0.01$) and ($P < 0.05$).

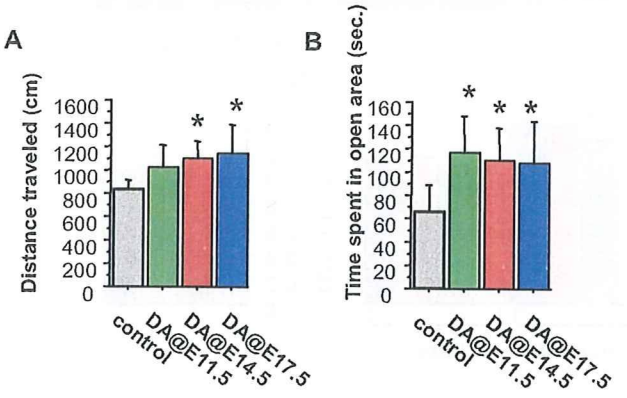

Fig. 5. Delayed effects on anxiety-related behavior (EP test) induced by prenatal exposure of DA.
A, Total distance travelled, and B, total time spent in open area in the elevated plus maze apparatus (mean ± S.E.M.). Asterisk (*) indicated significant difference compared to control ($P < 0.05$).

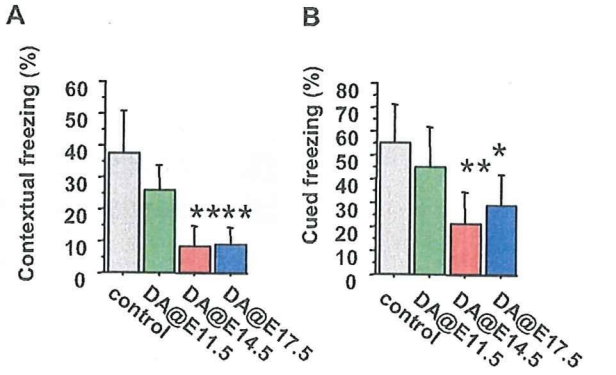

Fig. 6. Delayed effects on learning and memory (FZ test) induced by prenatal exposure of DA.
A, Contextual fear test and B, cued fear test. Memory performance is expressed as a mean percent duration of freezing responses (mean ± S.E.M.). Asterisk (**) and (*) indicated significant difference compared to control ($P < 0.01$) and ($P < 0.05$).

mice by using cytoskeletal marker. These findings indicated that the disorganization of brain was induced by the prenatal exposure of DA, and remained irreversibly up until the maturation period.

Among multiple endpoints of the behavioral test battery we used, serious deviances in anxiety-related behaviors of group C (DA@14.5) and D (DA@17.5) mice were observed. Mice in those groups showed low performances in adaptations for novel circumstances, i.e., strange and broad area in OF test, beamish place in LD test, high and narrow space in EP test. Additionally, we also found severe impairment of learning and memory. Although the low performances of memory task have been reported in rats with prenatal DA exposure (Levin *et al.*, 2005),

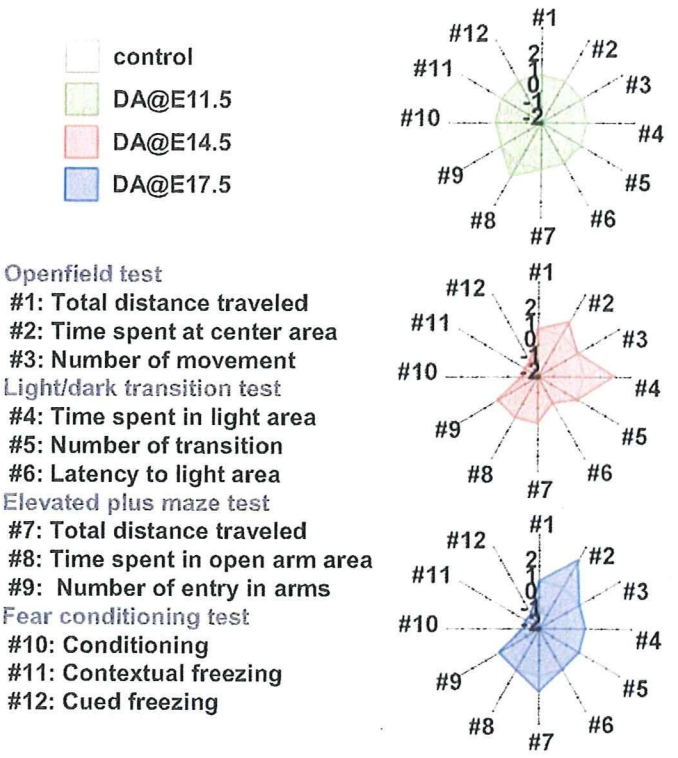

Fig. 7. Summary radar chart of the neurobehavioral battery test results. Radial axis indicates the direction (increase or decrease) of the deviation, and the p value of the endpoints compared to the control (+1 and −1, $0.01 <= p < 0.05$, +2 and −2, $p < 0.01$). Regular dodecagon of radius 0 indicates no deviation from control.

we showed serious deviances about affective (emotional) behaviors additional to severe memory deficit.

In conclusion, we clearly indicated that the disturbance against the adequate neural activity during developmental period when glutamate receptors became active have induced delayed memory defect and unnatural adoptive behaviors that became monitorable at the maturation period in mice. The responsible foci deduced from these behavioral disturbances are the limbic cortex and hippocampus. Our morphological findings are consistent with the interpretation. A combination of neurobehavioral and pathomorphological analysis was shown to be an effective method to assess delayed neurotoxic effects which dose not induce immediate organic brain damage and related symptoms after exposure. Having adopted the hypothesis that exogenous stimuli to neural signaling systems during the development of the brain can be a cause of delayed anomaly of higher brain function, stimuli toward systems other than glutamate receptors should also induce such anomaly of different targets and symptoms in concert with the distribution of the corresponding receptor(s) in the developing brain. Such data on other system would be reported elsewhere.

ACKNOWLEDGMENTS

The authors thank Mr. Yusuke Furukawa and Ms. Maki Otsuka for technical support. This study was supported by Health Sciences Research Grants H17- -Kagaku- 001 from the Ministry of Health, Labour and Welfare, Japan.

This peer-reviewed article is based upon a lecture presented at the 35th Annual Meeting of Japanese Society of Toxicology, June 2008 in Tokyo under the theme of "Children's Toxicology", June 2008 in Tokyo.

REFERENCES

Bondy, S.C. and Campbell, A. (2005): Developmental neurotoxicology. J. Neurosci. Res., **81**, 605-612.

Chandrasekaran, A., Ponnambalam, G. and Kaur, C. (2004): Domoic acid-induced neurotoxicity in the hippocampus of adult rats. Neurotox. Res., **6**, 105-117.

Cohen-Cory, S. (2002): The developing synapse: construction and

modulation of synaptic structures and circuits. Science, **298**, 770-776.

Dakshinamurti, K., Sharma, S.K., Sundaram, M. and Watanabe, T. (1993): Hippocampal changes in developing postnatal mice following intrauterine exposure to domoic acid. J. Neurosci., **13**, 4486-4495.

Fonta, C., Chappert, C. and Imbert, M. (2000): Effect of monocular deprivation on NMDAR1 immunostaining in ocular dominance columns of the marmoset Callithrix jacchus. Vis. Neurosci., **17**, 345-352.

Greer, P.L. and Greenberg, M.E. (2008): From synapse to nucleus: calcium-dependent gene transcription in the control of synapse development and function. Neuron, **59**, 846-860.

Gu, Q.A., Bear, M.F. and Singer, W. (1989): Blockade of NMDA-receptors prevents ocularity changes in kitten visual cortex after reversed monocular deprivation. Brain Res. Dev. Brain Res., **47**, 281-288.

Levin, E.D., Pizarro, K., Pang, W.G., Harrison, J. and Ramsdell, J.S. (2005): Persisting behavioral consequences of prenatal domoic acid exposure in rats. Neurotoxicol. Teratol., **27**, 719-725.

Luján, R., Shigemoto, R. and López-Bendito, G. (2005): Glutamate and GABA receptor signalling in the developing brain. Neuroscience, **130**, 567-580.

Manent, J.B., Demarque, M., Jorquera, I., Pellegrino, C., Ben-Ari, Y., Aniksztejn, L. and Represa, A. (2005): A noncanonical release of GABA and glutamate modulates neuronal migration. J Neurosci., **25**, 4755-4765.

Matsugami, T.R., Tanemura, K., Mieda, M., Nakatomi, R., Yamada, K., Kondo, T., Ogawa, M., Obata, K., Watanabe, M., Hashikawa, T. and Tanaka, K. (2006): Indispensability of the glutamate transporters GLAST and GLT1 to brain development. Proc. Natl. Acad. Sci. USA, **103**, 12161-12166.

Maucher, J.M. and Ramsdell, J.S.(2007): Maternal-fetal transfer of domoic acid in rats at two gestational time points. Environ Health Perspect., **115**, 1743-1746.

Miller, R.H. and Mi, S. (2007): Dissecting demyelination. Nat. Neurosci., **10**, 1351-1354.

Ooi, L. and Wood, I.C. (2008): Regulation of gene expression in the nervous system. Biochem. J., **414**, 327-341.

Pulido, O.M. (2008): Domoic acid toxicologic pathology: a review. Mar. Drugs, **6**, 180-219.

Rice, D. and Barone, S.Jr. (2000): Critical periods of vulnerability for the developing nervous system: evidence from humans and animal models. Environ. Health Perspect., **108**, 511-533.

Tanemura, K., Murayama, M., Akagi, T., Hashikawa, T., Tominaga, T., Ichikawa, M., Yamaguchi, H. and Takashima, A. (2002): Neurodegeneration with tau accumulation in a transgenic mouse expressing V337M human tau. J Neurosci., **22**, 133-141.

Tanemura, K., Ogura, A., Cheong, C., Gotoh, H., Matsumoto, K., Sato, E., Hayashi, Y., Lee, H.W. and Kondo, T. (2005): Dynamic rearrangement of telomeres during spermatogenesis in mice. Dev. Biol., **281**, 196-207.

Tatebayashi, Y., Miyasaka, T., Chui, D.H., Akagi, T., Mishima, K., Iwasaki, K., Fujiwara, M., Tanemura, K., Murayama, M., Ishiguro, K., Planel, E., Sato, S., Hashikawa, T. and Takashima, A. (2002): Tau filament formation and associative memory deficit in aged mice expressing mutant (R406W) human tau. Proc. Natl. Acad. Sci. USA, **99**, 13896-13901.

Tryphonas, L. and Iverson, F. (1990): Neuropathology of excitatory neurotoxins: the domoic acid model. Toxicol Pathol., **18**, 165-169.

Wiesel, T.N. (1982): Postnatal development of the visual cortex and the influence of environment. Nature, **299**, 583-591.

J. Biochem. 2010;147(3):353–360 doi:10.1093/jb/mvp169

JB THE JOURNAL OF BIOCHEMISTRY

Suppression of AhR signaling pathway is associated with the down-regulation of UDP-glucuronosyltransferases during BBN-induced urinary bladder carcinogenesis in mice

Received August 18, 2009; accepted October 15, 2009; published online October 29, 2009

Katsuyuki Iida[1,2], Junsei Mimura[3], Ken Itoh[3,*], Chikara Ohyama[4], Yoshiaki Fujii-Kuriyama[5], Toru Shimazui[1], Hideyuki Akaza[1] and Masayuki Yamamoto[2,6,†]

[1]Department of Urology, Institute of Clinical Medicine; [2]Center for TARA and JST-ERATO Environmental Response Project, University of Tsukuba, 1-1-1 Tennoudai, Tsukuba 305-8577; [3]Department of Stress Response Science; [4]Department of Urology, Hirosaki University Graduate School of Medicine, 5 Zaifu-cho, Hirosaki 036-8562; [5]Center for TARA and JST-SORST, University of Tsukuba, 1-1-1 Tennoudai, Tsukuba, 305-8577; and [6]Departement of Medical Biochemistry, Tohoku University Graduate School of Medicine, 2-1 Seiryo-cho, Aoba-ku, Sendai 980-8575, Japan

*Ken Itoh, Department of Stress Response Science, Hirosaki University, Graduate School of Medicine, 5 Zaifu-cho, Hirosaki 036-8562, Japan, Tel.: +81 172 39 5158, Fax: +81 172 39 5158, email: itohk@cc.hirosaki-u.ac.jp

†Masayuki Yamamoto, Department of Medical Biochemistry, Tohoku University, Graduate School of Medicine, 2-1 Seiryo-cho, Aoba-ku, Sendai 980-8575, Japan, Tel.: +81 22 717 8088, Fax: +81 22 717 8090, email: masi@mail.tains.tohoku.ac.jp

Down-regulation of carcinogen detoxifying enzymes might be a critical factor in tumour formation by increasing the carcinogen concentration in the target organ. Previous reports revealed that the expression of *UGT1A* mRNA is either lost or decreased in certain human cancer tissues, including urinary bladder cancer. To elucidate this down-regulation mechanism, we used an *N*-nitrosobutyl (4-hydroxybutyl) amine (BBN)-induced mouse urinary bladder carcinogenesis model. Similar to human cancer, the expressions of *Ugt1a6*, *Ugt1a9* and total *Ugt1a* mRNA in the BBN-induced bladder cancer were markedly decreased compared with those of normal mice. BBN down-regulated the basal *Ugt1a* mRNA expression in a time-dependent manner and this was reversible in the first 2 weeks of BBN treatment. However, after 4 weeks of BBN treatment the repression became persistent after the cessation of BBN treatment. Aryl hydrocarbon receptor (AhR) regulates the constitutive and inducible expression of *Ugt1a* mRNA. We found that the constitutive *Ugt1a* mRNA expression is decreased in the bladder of AhR knockout (KO) mice. Furthermore, BBN-induced *Ugt1a* down-regulation was lost in AhR KO mice, and the canonical AhR target gene *Cyp1a1* was similarly down-regulated by BBN in the bladder. These results demonstrate that BBN repressed *Ugt1a* mRNA expression *via* suppression of AhR signaling pathway during BBN-induced carcinogenesis.

Keywords: UDP-glucuronosyltransferase/urinary bladder carcinogenesis/AhR.

Abbreviations: AhR, Aryl hydrocarbon receptor; BBN, *N*-nitrosobutyl (4-hydroxybutyl) amine; Cyp1a1, cytochrome P450, family 1, subfamily a, polypeptide 1; Gstp1, Glutathione *S*-transferase, placental isoform 1; 3-MC, 3-methylcholanthrene; PAH, polycyclic aromatic hydrocarbon; UGT, UDP-glucuronosyltransferase.

Down-regulation of carcinogen detoxifying enzymes in target organs is likely to play a critical role in chemically induced carcinogenesis by leading to an increased local concentration of carcinogens (*1–5*). UDP-glucuronosyltransferases (UGTs) contribute to cellular detoxification through their glucuronidation of potentially toxic carcinogens and xenobiotics (*6–8*) and are thereby key players in the defense mechanism against chemical-induced carcinogenesis (*9*) and teratogenesis (*10*). Carcinogens, such as aromatic amines and polycyclic aromatic hydrocarbons (PAHs), are detoxified by conjugation with glutathione or UDP-glucuronic acid (*11, 12*). The 19 human *UGT* cDNAs identified so far include nine *UGT1A* genes encoded by a single *UGT1A* locus on chromosome 2 and 10 individually encoded *UGT2* genes on chromosome 4 (*13*). *UGT1A* genes mainly catalyse the glucuronidation of aromatic amines and PAHs (*13*) and down-regulation of *UGT1A* gene expression has been associated with liver, digestive tract and urinary bladder tumors in human (*1–4*).

Each *Ugt1a* gene consists of a gene specific protein-encoding first exon and 2–5 common exons. Gene-specific promoters 5′ of the first exons control the specific expression of individual *Ugt1a* genes. Basal *Ugt1a* mRNA expression is regulated tissue-specifically by several transcription factors, such as hepatocyte nuclear factor 1 and CAAT-enhancer binding protein (*14, 15*). On the other hand, the inducible expression of *Ugt1a* mRNA is regulated by several xenobiotic receptors including pregnenolone X receptor, constitutive androstane receptors, peroxisome proliferators-activated receptors, liver X receptor, aryl hydrocarbon receptor (AhR) and NF-E2-related factor 2 (Nrf2) (*16–20*).

The AhR regulates inducible expression of both phase 1 and phase 2 drug metabolizing enzyme genes (*21, 22*). AhR is usually sequestered in the cytoplasm in association with Hsp90, p23 and XAP2/ARA9. Upon binding to halogenated or polycyclic aromatic hydrocarbons, such as 2,3,7,8-tetrachlorodibenzo-*p*-dioxin (TCDD) and 3-methylcholanthrene (3-MC),

respectively, AhR translocates into the nucleus, and dimerizes with its partner molecule, Arnt (AhR nuclear translocator), and then binds to its cognate enhancer sequences called XREs in the regulatory region of *Ugt1a*, *Cyp1a1* and glutathione S-transferase a1 (*Gsta1*) genes (*23–25*). Chen *et al.* (*26*) recently showed that the AhR controls *UGT1A* gene expression more profoundly than was previously anticipated from transgenic mouse studies with the human *UGT1A* locus. Although a distribution of XREs occurs immediately upstream of the *UGT1A1*, *UGT1A6* and *UGT1A9* first exons, TCDD treatment activated the expression of all the human *UGT1A* genes in small and large intestines, suggesting that AhR regulates the transcriptional activity of the whole *UGT1A* locus (*26*). Nrf2 also plays important role in *Ugt1a* gene expression. Nrf2 is activated by electrophiles, such as oltipraz and sulforaphane, and coordinately regulates expression of phase 2 drug metabolizing enzymes including Ugt1a6 and Gsts (*27*, *28*).

Oral administration of *N*-nitrosobutyl(4-hydroxybutyl)amine (BBN) to rodents induced cancer specifically in urinary bladder (*29*). BBN itself is either metabolized by alcohol/aldehyde dehydrogenase-mediated oxidation to yield *N*-nitrosobutyl (3-carboxypropyl)amine (BCPN) or by UGT to form BBN-glucuronide conjugate which is easily excreted from bladder (*30*). If BBN or BCPN are metabolized through the α-hydroxylation pathway and chemically cleaved, their corresponding reactive species of alkylcarbonium ion are generated. Carbonium ion binds covalently to DNA and enhances carcinogenesis in uroepithelial cells (*31*, *32*). We previously demonstrated that *Ugt1a* mRNA expression is specifically down-regulated in the mouse urinary bladder after BBN exposure (*27*). This may reduce the local glucuronidation activity against carcinogens, allowing their accumulation and consequent promotion of DNA mutations. In this study, we used a BBN-induced urinary bladder carcinogenesis model to elucidate the mechanism of *Ugt1a* mRNA down-regulation during carcinogenesis.

Materials and methods

Animals and reagents

BBN was purchased from Tokyo Kasei (Tokyo, Japan) and 3-MC was bought from Sigma Chemical Co. (St Louis, MO, USA). Nrf2-deficient mice of an ICR/129SV background (*28*) were backcrossed for nine generations with C57BL/6J mice acquired from CLEA Japan (Tokyo, Japan). The *Ahr*$^{-/-}$ mice (*33*) have been backcrossed to C57BL/6J mice for seven generations. Mice were housed in stainless steel cages in an animal room maintained at 24 ± 2°C and with a 12 h light/dark cycle. Mice were fed a purified AIN-76A diet (Oriental MF; Oriental Yeast Co., Tokyo) and given water *ad libitum*. BBN was dissolved in tap water to the set concentrations and supplied *ad libitum* in dark bottles. 3-MC was dissolved in corn oil to a concentration of 4 mg/ml. Mice were treated with a single injection of 80 mg/kg of 3-MC intraperitoneally.

RNA blot analysis

After the experimental period, mice were analysed by autopsy. Total RNAs from whole urinary bladders or cancer lesions were extracted with Isogen (Nippon Gene, Toyama) according to the manufacturer's instructions. Total RNAs (10 μg) were separated by 1.5% agarose gel electrophoresis containing 2.2 M formaldehyde and transferred to a nylon membrane. Membranes were hybridized with the ^{32}P-labelled gene-specific cDNA probes and washed with the stringent washing conditions (final wash was done by 0.1% SSC, 0.1% SDS solution for 30 min at 55°C). cDNA probes for *Ugt1a6*, *Ugt1a9* and total *Ugt1a* have been described (*27*) and a cDNA probe for *Gstp1* was kindly provided by Dr Kimihiko Satoh.

Immunoblot analysis of mAhR

Total proteins from whole mouse bladders were homogenized on ice in 500 μl of RIPA lysis buffer [PBS (pH 7.4) containing 1% Nonidet P-40, 0.5% sodium deoxycholate, 0.1% SDS, 100 μg/ml phenylmethylsulfonyl fluoride, 5 μg/ml aprotinin, 10 μg/ml leupeptin, 10 μg/ml pepstatin, 1 mM sodium ortho-vanadate and 1 mM DTT]. After incubation for 30 min on ice, homogenates were centrifuged at maximum speed (15 000 r.p.m.) in a microcentrifuge for 30 min at 4°C. Protein concentrations of the supernatants were determined by Coomassie Plus Protein Assay Reagent (Pierce). Proteins were separated by 10% SDS–PAGE and electro-transferred onto an Immobile membrane (Millipore, Bedford, MA, USA). The membrane was incubated for 8 h at 4°C with anti-AhR antibody (SA-210; BIOMOL, PA, USA) diluted 1 : 200 in TBST (TBS plus 0.05% Tween-20). Immunoreactive proteins were detected using horseradish peroxidase-conjugated anti-IgG antibody and ECL (Amersham Biosciences).

Statistical analyses

Data were expressed as means ± SEM. The student's *t*-test was used to determine the statistical differences among groups. A $P < 0.05$ was interpreted as statistically significant.

Results

Reduced Ugt1a mRNA expression in BBN-induced mouse urinary bladder cancer

We previously found that BBN dose-dependently down-regulated *Ugt1a* mRNA expression after 2 weeks of BBN exposure in a manner independent of Nrf2 (*27*). In addition, decreased *UGT1A* mRNA expression has been reported in several human cancers. To examine whether *Ugt1a* mRNA expression is decreased in BBN-induced urinary bladder cancer, we examined the mRNA expressions of *total Ugt1a* and its representative isoforms *Ugt1a6* and *Ugt1a9* in BBN-induced urinary bladder carcinoma. For this purpose, mice were treated with 0.05% BBN for 12 weeks and *Ugt1a* mRNA expressions in the urinary bladder were analysed 10 weeks after ceasing treatment. Unlike untreated mice, those administered BBN suffered from apparent urinary bladder cancer, with bladder lesions that were nodular rather than papillary in shape. The expressions of *Ugt1a6*, *Ugt1a9* and *total Ugt1a* mRNAs in the urinary bladders of BBN-treated mice were significantly decreased by 87.7, 98.2 and 80.0%, respectively, compared to those of control mice (Fig. 1). On the other hand, *Gstp* mRNA expression was increased by 290.3%, indicating that the down-regulation of *Ugt1a* mRNA expression in the cancerous urinary bladder is specific amongst phase 2 genes.

Persistent down-regulation of Ugt1a mRNA after prolonged BBN exposure

In order to examine the mechanism of *Ugt1a* suppression in more detail, we analysed *Ugt1a* mRNA expression after exposure to 0.05% BBN for 0, 3, 7 and 14 days (Fig. 2A and B). The expressions of *Ugt1a6*, *Ugt1a9* and *total Ugt1a* mRNAs were down-regulated

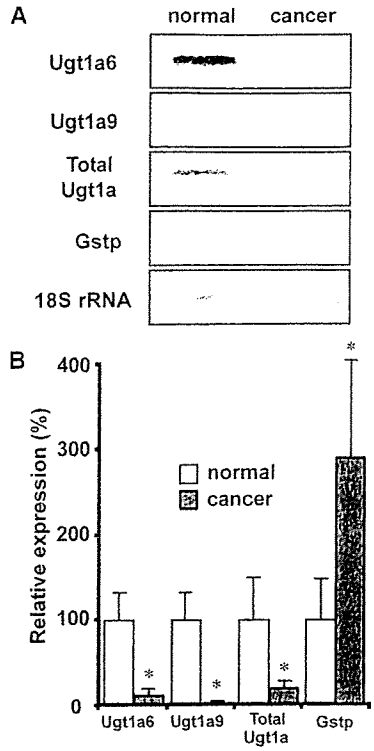

Fig. 1 The expressions of *Ugt1a6*, *Ugt1a9* and total *Ugt1a* mRNAs in BBN-induced urinary bladder cancer compared with those in normal urinary bladder. Mice were treated with vehicle (normal) or 0.05% BBN (cancer) for 12 weeks. Ten weeks after the cessation of BBN treatment, the expression of *Ugt1a* mRNA in the urinary bladder was analysed. The band intensities of the RNA blot (**A**) were quantified by densitometric analysis and the mRNA levels of phase 2 genes were normalized by *18S rRNA* levels. The expression level of each phase 2 gene in vehicle-treated mice was arbitrarily set to 100 and that of the BBN-treated mice is shown as a percentage of this control (**B**). The means from four mice are presented with the SEM ($n=4$). $*P \leq 0.05$ compared with untreated wild-type mice.

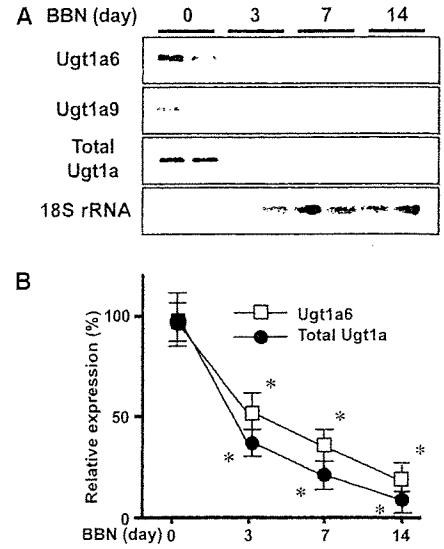

Fig. 2 Effect of BBN on *Ugt1a* mRNA expression in the urinary bladder. Mice were treated with 0.05% BBN or vehicle for 0, 3, 7 and 14 days, then urinary bladder RNA were extracted for RNA blot analysis. The band intensities of the RNA blot (**A**) were quantified by densitometric analysis and expression levels of phase 2 genes were normalized by *18S rRNA* levels. The mRNA level of each *Ugt1a* gene in untreated mice was arbitrarily set to 100 and that of BBN-treated mouse is shown as a percentage of this control (**B**). The means from four mice are presented with the SEM ($n=4$). $*P \leq 0.05$ compared with untreated wild-type mice.

by BBN treatment as early as 3 days and decreased in a time-dependent manner until 14 days.

It is known that gene expression is altered irreversibly after cancerous transformation. Therefore, we examined whether the down-regulation of *Ugt1a* mRNA expression is reversible after the cessation of BBN treatment. For this purpose, mice were treated with 0.05% BBN for 2 weeks and *Ugt1a* mRNA expression in the urinary bladder was examined 1, 2, 4, 7 and 14 days after the cessation of BBN treatment. Suppression of *Ugt1a6*, *Ugt1a9 and total Ugt1a* mRNA levels was maintained up to 4 days after the interruption of BBN treatment (Fig. 3A). However, 7 days after ceasing BBN administration, *Ugt1a* mRNA expression increased to a level exceeding those of untreated mice, demonstrating the reversibility of the process after a short period (*i.e.* 2 weeks) of carcinogen treatment.

But what of longer term BBN exposure? Mice were treated with 0.05% BBN for 2, 4, 6, 9 and 12 weeks and the expression of *Ugt1a6 and* total *Ugt1a* mRNAs was examined 7 days after discontinuing BBN treatment at each time point (Fig. 3B). We found that the expression of *Ugt1a6 and* total *Ugt1a* mRNAs did not fully recover after the mice were treated with BBN for 4 weeks or longer. Thus, chronic BBN exposure of greater than 2 weeks resulted in the persistent down-regulation of *Ugt1a* mRNA expression.

Ugt1a down-regulation by BBN treatment is not observed in the AhR KO mouse bladder

Ugt1a mRNA expression is regulated by multiple transcription factors, such as Nrf2 and the AhR (*16*, *17*). To elucidate if the Nrf2 or AhR pathway is responsible for the down-regulation of *Ugt1a* mRNA expression by BBN, we analyzed *Ugt1a* mRNA expression in the urinary bladders of $Nrf2^{-/-}$ and $Ahr^{-/-}$ mice after exposure to 0.05% BBN for 2 weeks (Fig. 4A and B). Importantly, the basal expressions of *Ugt1a6*, *Ugt1a9* and *total Ugt1a* mRNAs in $Ahr^{-/-}$ mice were significantly decreased by 80.0%, 92.8% and 83.8%, respectively, compared with those of wild-type mice. On the other hand, *Ugt1a6*, *Ugt1a9* and *total Ugt1a* mRNA expressions in $Nrf2^{-/-}$ mice were not significantly altered compared with those of wild-type mice. After BBN treatment, *Ugt1a* mRNA expression was significantly decreased by >80% in both $Nrf2^{-/-}$ and wild-type mice. However, in $Ahr^{-/-}$ mice, the constitutively low *Ugt1a* mRNA expression was not further reduced upon BBN exposure.

Further confirmation that the AhR indeed regulates *Ugt1a* mRNA expression in the urinary bladder was provided by treating both wild-type and $Ahr^{-/-}$ mice with the AhR activator 3-MC. The expressions of *Ugt1a* and *Cyp1a1* mRNAs were measured 48 h post-intraperitoneal injection of 3-MC (Fig. 4*C*). The expressions of *Ugt1a6*, *Ugt1a9*, *total Ugt1a* and *Cyp1a1* mRNAs in wild-type mice were significantly

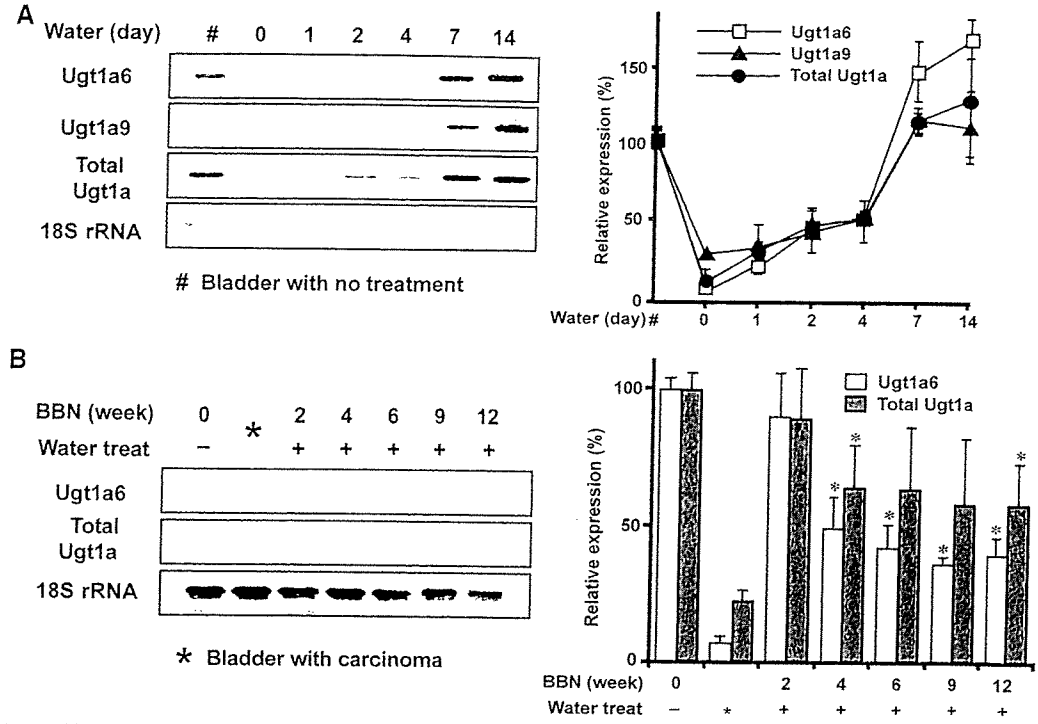

Fig. 3 Expression of *Ugt1a* mRNAs after the cessation of BBN treatment. (A) Mice were treated with 0.05% BBN for 2 weeks and total RNAs from the urinary bladders were examined for *Ugt1a* mRNA expression 1, 2, 4, 7 and 14 days after the cessation of BBN treatment. (B) Mice were treated with 0.05% BBN for 2, 4, 6, 9 and 12 weeks. Total RNAs from the urinary bladders were examined for *Ugt1a* mRNA expression 7 days after the cessation of BBN treatment at each time point. The band intensities of the RNA blots (left panels) were quantified by densitometry and the expression levels of *Ugt1a* mRNAs were normalized by *18S rRNA* levels. The expression level of *Ugt1a* mRNA in untreated mice was arbitrarily set to 100 and that of the BBN-treated mouse is shown as a percentage of this control (right panels). Values are presented as means ± SEM ($n=4$). $^*P \leq 0.05$ compared with untreated wild-type mice.

increased by 157.7, 143.8, 194.0 and 1509.0%, respectively, after 3-MC treatment. However, the constitutive expression of these genes was decreased in $Ahr^{-/-}$ mice and induction by 3-MC was lost. These results clearly demonstrate a similar regulation of mRNA expression under the influence of the AhR between *Ugt1a* and *Cyp1a1* genes in the urinary bladder.

Expression of AhR protein and the activity of the AhR pathway after BBN treatment

To examine the effect of BBN on AhR activity, we measured the expression of AhR protein and the AhR target gene expression in the urinary bladder after 2 weeks of BBN treatment. Immunoblot analysis using whole urinary bladder extracts demonstrated that BBN treatment significantly increased AhR protein in a dose-dependent manner (Fig. 5A). Because RNA blot analysis showed that the *Ahr* mRNA level was not increased by BBN treatment (data not shown), AhR protein translation rate or stability may be increased by BBN treatment. We evaluated the AhR target gene expression after BBN treatment by measuring *Cyp1a1* mRNA expression by RNA blot analysis. Mice were treated with 0.01, 0.05 and 0.1% BBN for 2 weeks and the expression of *Cyp1a1* mRNA in urinary bladder was examined. The results revealed that BBN treatment decreased *Cyp1a1* mRNA expression. These results indicated that AhR signaling is suppressed by BBN treatment although AhR protein itself is increased by BBN (Fig. 5B).

AhR activity is repressed in BBN-induced cancerous tissue

Because AhR protein is increased but its activity may be suppressed by BBN, we next analyzed AhR protein level and *Cyp1a1* expression in cancerous tissue. Mice were administered BBN for 12 and then with water for 10 weeks following the stoppage of BBN treatment, *Cyp1a1* mRNA expression in the cancerous tissues was examined. RNA blot analysis demonstrated a decrease in *Cyp1a1* mRNA expression similar to the decrease in *Ugt1a* mRNA expression, indicating the persistent repression of AhR signaling in cancerous urinary bladder (Fig. 5C). Consistent with the results of Fig. 5A, the expression of AhR protein in whole bladder extract remained elevated even 10 weeks after ending BBN treatment (Fig. 5D). Thus, BBN suppresses AhR signaling pathway in cells, hence repressing *Ugt1a* mRNA expression during BBN-induced carcinogenesis.

Discussion

Our study established that *Ugt1a* mRNA expression is markedly decreased in BBN-induced urinary bladder cancer, with the decreased expression commencing during the early phase of continuous BBN administration. In *Ahr* KO mice, although the expression of

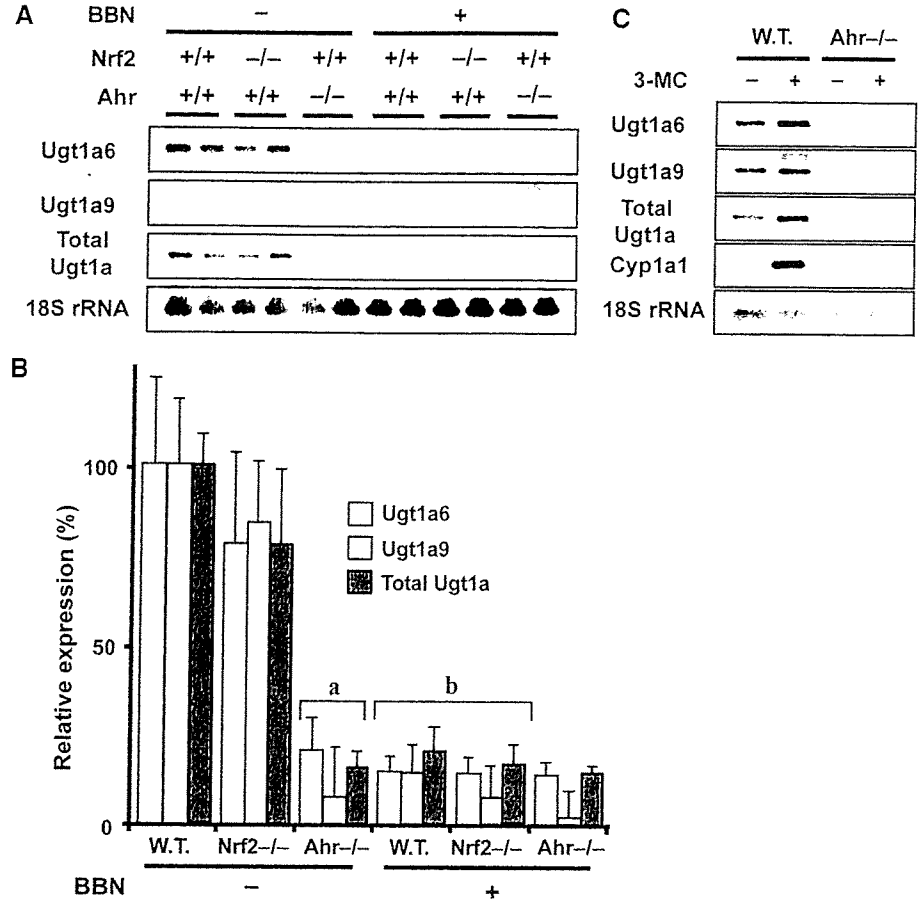

Fig. 4 Role of AhR on *Ugt1a* mRNA expression in the urinary bladder. (**A**) Effect of *Ahr* or *Nrf2* gene deletion on *Ugt1a* mRNA expression. Wild-type, $Nrf2^{-/-}$ and $Ahr^{-/-}$ mice were treated with 0.05% BBN for 2 weeks and the expression levels of *Ugt1a* mRNAs in the urinary bladders were examined. (**B**) The expression level of *Ugt1a* mRNA in untreated wild-type mice was arbitrarily set to 100 and that of each mouse as indicated in the figure is shown as a percentage of this control. (**A**) $P \leq 0.05$ compared with untreated wild-type mice. (**B**) $P \leq 0.05$ compared with untreated mice of the same genotype. (**C**) Effect of 3-MC on *Ugt1a* mRNA expression in the urinary bladder. Wild-type and $Ahr^{-/-}$ mice were injected intraperitoneally with 80 mg/kg of 3-MC. After 48h, the expressions of *Ugt1a* mRNAs and the *Cyp1a1* mRNA were examined by RNA blot analysis.

Ugt1a mRNA was constitutively low, BBN treatment did not further suppress *Ugt1a* mRNA expression. BBN appears to down-regulate *Ugt1a* mRNA expression *via* the suppression of AhR-dependent signaling pathway. These results indicate that the potent carcinogen BBN facilitates carcinogenesis by repressing the expression of AhR-dependent detoxification genes.

Our current hypothesis of *Ugt1a* mRNA down-regulation during BBN-induced urinary bladder carcinogenesis is summarized in Fig. 6. Under normal conditions, when the urinary bladder is continually exposed to urine, the basal expression of *Ugt1a* mRNA is up-regulated by the AhR that is activated by urinary ligands such as indigos (*34*). BBN-treatment increases AhR protein level in the cells, but the *Ugt1a* mRNA expression is suppressed by BBN-treatment. After long BBN exposure, the down-regulation of *Ugt1a* mRNA becomes persistent and this may allow for the accumulation of carcinogen and consequently predispose the urinary bladder to carcinogenesis.

It is known that BBN is metabolized by the conjugation of glucuronic acid in rat (*30*). However, UGT isozymes responsible for BBN-glucuronidation are not clear at present. We previously demonstrated that Nrf2 activator oltipraz induce BBN-glucuronidation in an Nrf2-dependent manner in mouse liver (*27*). As Nrf2 regulates a battery of *Ugt1a* as well as *Ugt2b* mRNA expression, we surmise that either of these Ugt family members probably catalyse BBN glucuronidation in mice (*35*, *36*).

Several studies have clarified the mechanism of gene silencing in cancer. For example, methylation of the 5′ CpG island is thought to play an important role in the inactivation of tumor suppressor genes in cancer. The *GSTP1* gene is the major GST isoform expressed in normal human prostate and is silenced in the majority of prostate tumors by the hypermethylation of CpG islands in the 5′ regulatory region (*5*). Similarly, expression of *UGT1A* mRNA is also down-regulated in the early stages of human liver and biliary carcinogenesis, but the mechanism has not been elucidated (*1*). To determine the mechanism of down-regulation of *Ugt1a* mRNA, we evaluated methylation of the *Ugt1a6* gene promoter in mouse cancerous urinary bladder. However, we failed to detect methylation of CpG in the promoter between −1.2 kb and 0.1 kb (data not shown).

It is important to note that BBN does not repress *Ugt1a* mRNA expression in the liver. Since BBN is metabolized to its reactive species only in the urinary bladder, it might be the reactive metabolites of BBN that are repressing the AhR. The repression mechanism was examined using primary culture of urinary bladder epithelial cells, but we found that neither BBN nor BCPN down-regulated basal *Ugt1a* mRNA expression. This might reflect the fact that the AhR does not contribute to basal *Ugt1a* mRNA expression *in vitro*, because of the absence of its urinary ligands. In contrast to the urinary bladder, transcription factors other than the AhR may contribute to the basal expression of *Ugt1a* mRNA in the liver. If this is the case, even if BBN represses liver AhR, it would not repress the expression of *Ugt1a mRNA*. Clarification of these possibilities requires further study.

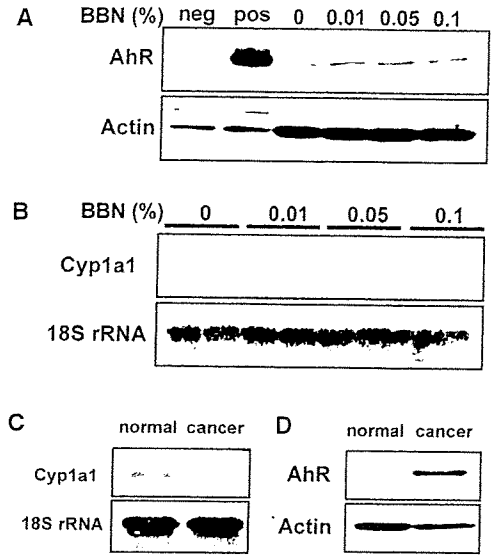

Fig. 5 The effect of BBN treatment on the AhR pathway. (A) Effect of BBN on the expression of the AhR in the urinary bladder. Mice were treated with vehicle, or 0.01%, 0.05%, 0.1% BBN for two weeks. Total cell extracts of the urinary bladders were examined by immunoblot analysis using anti-AhR antibody. neg, the total cell extract of COS-7 cells transfected with empty vector; posi, the total cell extract of COS-7 cells transfected with AhR expression vector. anti-β-actin antibody was used as a loading control. (B) Effect of BBN on *Cyp1a1* mRNA expression. Mice were treated with 0.01, 0.05 and 0.1% BBN or vehicle for two weeks and total RNAs from the urinary bladders were examined for the expression of *Cyp1a1* gene. (C) Down-regulation of *Cyp1a1* mRNA expression in urinary bladder cancer. Mice were treated with vehicle (normal) or 0.05% BBN (cancer) for 12 weeks and then with water for 10 weeks. *Cyp1a1* mRNA expression in the urinary bladder was examined by RNA blot analysis. (D) AhR protein expression in urinary bladder cancer. Mice were treated with vehicle (normal) or 0.05% BBN (cancer) for 12 weeks and then with water for 10 weeks. Total cell extracts of cancerous urinary bladders were examined by immunoblot analysis using anti-AhR antibody. Anti-β-actin antibody was used as a loading control.

It is known that ligand-coupled AhR is rapidly degraded by the ubiquitin–proteasome system (UPS) (*37*, *38*). Several studies reported that many transactivators possess rapid-turnover characteristics, indicating an association between transcriptional activation and protein degradation (*39*). Indeed, the proteolysis of some transcriptional activators by the UPS can stimulate transcription (*40*, *41*). However, since the proteasome inhibitors MG132 and lactacystin block AhR degradation by TCDD, but lead to an enhancement of AhR transcriptional activity, proteolysis *per se* may not be essential for the transactivation activity of the AhR (*37*, *38*). Recently, Chen *et al.* (*42*) demonstrated that MEK inhibitor U0126 stabilizes the AhR and increases its steady-state levels, but also diminishes the ability of the activated AhR to induce *Cyp1a1* in response to TCDD. In that paper, the authors speculated that Erk induces a conformational change that provokes both transcriptional activation and degradation of the AhR. Collectively, these studies argue that degradation of the cellular AhR is not necessarily a requirement for transcription, but a property of the ligand-activated form of the receptor. It is not clear whether the same phenomenon occurs in BBN-treated bladder, but an interesting possibility might be that BBN inhibits Erk in the urinary bladder.

The repression of *Ugt1a* mRNA expression becomes persistent after longer BBN exposure (i.e. after 4 weeks or longer exposure), and the inhibition of AhR signaling pathway and the repression of *Ugt1a* mRNA was also observed in the cancerous urinary bladder tissue, that is even 10 weeks after the cessation of BBN treatment (Fig. 5). Although it is not clear whether the inhibition mechanisms of AhR signaling pathway are identical in the non-cancerous and cancerous tissues, these results suggest that persistent

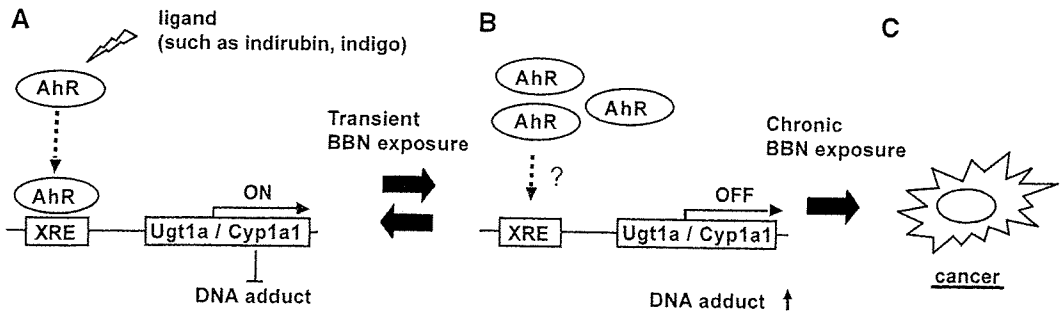

Fig. 6 The hypothetical mechanism of *Ugt1a* mRNA down-regulation during urinary bladder carcinogenesis. (A) Normally, the basal mRNA expressions of *Ugt1a* and *Cyp1a1* are mediated by the AhR that is constitutively activated by exposure to AhR ligands in the urine. (B) The AhR signaling pathway is repressed either by BBN or BBN metabolites by yet unidentified mechanisms, which down-regulates the mRNA expressions of *Ugt1a* and *Cyp1a1*. (C) If BBN exposure has been transient, the expression of *Ugt1a* mRNA swiftly recovers to normal levels. However, after a long exposure to BBN of >4 weeks, the down-regulation becomes persistent.

inhibition of *Ugt1a* expression *via* inhibition of AhR signaling pathway play an important role in carcinogenesis. Further studies will be required to find out how BBN or its metabolites inhibit AhR signaling pathway in the bladder.

This is the first report demonstrating that suppression of AhR signaling pathway is associated with the down-regulation of *Ugt1a* mRNA during urinary bladder carcinogenesis. Continuous exposure to carcinogen causes persistent repression of *Ugt1a* mRNA expression and may induce carcinogenesis. Conversely, we previously reported that Nrf2 activation antagonizes the BBN-induced repression of urinary *Ugt1a* mRNA expression (*27*). Thus, Nrf2 activation by dietary anticarcinogenic vegetables and fruits not only induces phase 2 expression, but also counteracts carcinogen-mediated repression of *Ugt1a* mRNA expression, thereby protecting the urinary bladder from carcinogenesis.

Acknowledgements

We thank Drs Atsushi Maruyama, Nobuhiko Harada and Tania O'Connor for their help and critical reading of the manuscript.

Funding

This work was supported in part by grants from JST-ERATO, JSPS, the Ministry of Education, Science, Sports and Technology, the Ministry of Health, Labor and Welfare, and the Naito Foundation.

Conflict of interest

None declared.

References

1. Strassburg, C.P., Manns, M.P., and Tukey, R.H. (1997) Differential down-regulation of the UDP-glucuronosyltransferase 1A locus is an early event in human liver and biliary cancer. *Cancer Res.* **57**, 2979–2985
2. Strassburg, C.P., Nguyen, N., Manns, M.P., and Tukey, R.H. (1998) Polymorphic expression of the UDP-glucuronosyltransferase UGT1A gene locus in human gastric epithelium. *Mol. Pharmacol.* **54**, 647–654
3. Giuliani, L., Gazzaniga, P., Caporuscio, F., Ciotti, M., Frati, L., and Agliano, A.M. (2001) Can down-regulation of UDP-glucuronosyltransferases in the urinary bladder tissue impact the risk of chemical carcinogenesis? *Int. J. Cancer* **91**, 141–143
4. Giuliani, L., Ciotti, M., Stoppacciaro, A., Pasquini, A., Silvestri, I., De Matteis, A., Frati, L., and Aglianò, A.M. (2005) UDP-glucuronosyltransferases 1A expression in human urinary bladder and colon cancer by immunohistochemistry. *Oncol. Rep.* **13**, 185–191
5. Nelson, C.P., Kidd, L.C., Sauvageot, J., Isaacs, W.B., De Marzo, A.M., Groopman, J.D., Nelson, W.G., and Kensler, T.W. (2001) Protection against 2-hydroxyamino-1-methyl-6-phenylimidazo[4,5-b]-pyridine cytotoxicity and DNA adduct formation in human prostate by glutathione S-transferase P1. *Cancer Res.* **61**, 103–109
6. Dutton, G.J. (1980) *Glucuronidation of Drugs and Other Compounds*. CRC Press, Boca Raton, FL
7. Burchell, B. and Coughtrie, M.W. (1989) UDP-glucuronosyltransferases. *Pharmacol. Ther.* **43**, 261–289
8. Burchell, B., Nebert, D.W., Nelson, D.R., Bock, K.W., Iyanagi, T., Jansen, P.L., Lancet, D., Mulder, G.J., Chowdhury, J.R., Siest, G., Tephly, T.R., and Mackenzie, P.I. (1991) The UDP glucuronosyltransferase gene superfamily: suggested nomenclature based on evolutionary divergence. *DNA Cell Biol.* **10**, 487–494
9. Vienneau, D.S., DeBoni, U., and Wells, P.G. (1995) Potential genoprotective role for UDP-glucuronosyltransferases in chemical carcinogenesis: initiation of micronuclei by benzo(a)pyrene and benzo(e)-pyrene in UDP-glucuronosyltransferase-deficient cultured rat skin fibroblasts. *Cancer Res.* **55**, 1045–1051
10. Kim, P.M., Winn, L.M., Parman, T., and Wells, P.G. (1997) UDP-glucuronosyltransferase-mediated protection against in vitro DNA oxidation and micronucleus formation initiated by phenytoin and its embryotoxic metabolite 5-(p-hydroxyphenyl)-5-phenylhydantoin. *J. Pharmacol. Exp. Ther.* **280**, 200–209
11. Ciotti, M., Lakshmi, V.M., Basu, N., Davis, B.B., Owens, I.S., and Zenser, T.V. (1999) Glucuronidation of benzidine and its metabolites by cDNA-expressed human UDP-glucuronosyltransferases and pH stability of glucuronides. *Carcinogenesis* **20**, 1963–1969
12. Filiadis, I. and Hrouda, D. (2000) Genetic factors in chemically-induced transitional cell bladder cancer. *BJU Int.* **86**, 794–801
13. Tukey, R.H. and Strassburg, C.P. (2000) Human UDP-glucuronosyltransferases: metabolism, expression, and disease. *Annu. Rev. Pharmacol. Toxicol.* **40**, 581–616
14. Auyeung, D.J., Kessler, F.K., and Ritter, J.K. (2003) Differential regulation of alternate UDP-glucuronosyltransferase 1A6 gene promoters by hepatic nuclear factor-1. *Toxicol. Appl. Pharmacol.* **191**, 156–166
15. Lee, Y.H., Sauer, B., Johnson, P.F., and Gonzalez, F.J. (1997) Disruption of the c/ebp alpha gene in adult mouse liver. *Mol. Cell. Biol.* **17**, 6014–6022
16. Chen, C., Staudinger, J.L., and Klaassen, C.D. (2003) Nuclear receptor, pregname X receptor, is required for induction of UDP-glucuronosyltranferases in mouse liver by pregnenolone-16 alpha-carbonitrile. *Drug Metab. Dispos.* **31**, 908–915
17. Xie, W., Yeuh, M.F., Radominska-Pandya, A., Saini, S.P., Negishi, Y., Bottroff, B.S., Cabrera, G.Y., Tukey, R.H., and Evans, R.M. (2003) Control of steroid, heme, and carcinogen metabolism by nuclear pregnane X receptor and constitutive androstane receptor. *Proc. Natl Acad. Sci. USA* **100**, 4150–4155
18. Verreault, M., Senekeo-Effenberger, K., Trottier, J., Bonzo, J.A., Bélanger, J., Kaeding, J., Staels, B., Caron, P., Tukey, R.H., and Barbier, O. (2006) The liver X-receptor alpha controls hepatic expression of the human bile acid-glucuronidating UGT1A3 enzyme in human cells and transgenic mice. *Hepatology* **44**, 368–378
19. Enomoto, A., Itoh, K., Nagayoshi, E., Haruta, J., Kimura, T., O'Connor, T., Harada, T., and Yamamoto, M. (2001) High sensitivity of Nrf2 knockout mice to acetaminophen hepatotoxicity associated with decreased expression of ARE-regulated drug metabolizing enzymes and antioxidant genes. *Toxicol. Sci.* **59**, 169–177
20. Auyeung, D.J., Kessler, F.K., and Ritter, J.K. (2003) Mechanism of rat UDP-glucuronosyltransferase 1A6 induction by oltipraz: evidence for a contribution of the Aryl hydrocarbon receptor pathway. *Mol. Pharmacol.* **63**, 119–127

21. Perdew, G.H. (1988) Association of the Ah receptor with the 90-kDa heat shock protein. *J. Biol. Chem.* **263**, 13802–13805
22. Pongratz, I., Mason, G.G., and Poellinger, L. (1992) Dual roles of the 90-kDa heat shock protein hsp90 in modulating functional activities of the dioxin receptor. Evidence that the dioxin receptor functionally belongs to a subclass of nuclear receptors which require hsp90 both for ligand binding activity and repression of intrinsic DNA binding activity. *J. Biol. Chem.* **267**, 13728–13734
23. Metz, R.P. and Ritter, J.K. (1998) Transcriptional activation of the UDP-glucuronosyltransferase 1A7 gene in rat liver by aryl hydrocarbon receptor ligands and oltipraz. *J. Biol. Chem.* **273**, 5607–5614
24. Fujisawa-Sehara, A., Sogawa, K., Yamane, M., and Fujii-Kuriyama, Y. (1987) Characterization of xenobiotic responsive elements upstream from the drug-metabolizing cytochrome P-450c gene: a similarity to glucocorticoid regulatory elements. *Nucleic Acids Res.* **15**, 4179–4191
25. Nebert, D.W., Roe, A.L., Dieter, M.Z., Solis, W.A., Yang, Y., and Dalton, T.P. (2000) Role of the aromatic hydrocarbon receptor and [Ah] gene battery in the oxidative stress response, cell cycle control, and apoptosis. *Biochem. Pharmacol.* **59**, 65–85
26. Chen, S., Beaton, D., Nguyen, N., Senekeo-Effenberger, K., Brace-Sinnokrak, E., Argikar, U., Remmel, R.P., Trottier, J., Barbier, O., Ritter, J.K., and Tukey, R.H. (2005) Tissue-specific, inducible, and hormonal control of the human UDP-glucuronosyltransferase-1 (UGT1) locus. *J. Biol. Chem.* **280**, 37547–37557
27. Iida, K., Itoh, K., Kumagai, Y., Oyasu, R., Hattori, K., Kawai, K., Shimazui, T., Akaza, H., and Yamamoto, M. (2004) Nrf2 is essential for the chemopreventive efficacy of oltipraz against urinary bladder carcinogenesis. *Cancer Res.* **64**, 6424–6431
28. Itoh, K., Chiba, T., Takahashi, S., ishii, T., Igarashi, K., Katoh, Y., Oyake, T., Hayashi, N., Satoh, K., Hatayama, I., Yamamoto, M., and Nabeshima, Y. (1997) An Nrf2/small Maf heterodimer mediates the induction of phase II detoxifying enzyme genes through antioxidant response elements. *Biochem. Biophys. Res. Commun.* **236**, 313–322
29. Ito, N., Hiasa, Y., Tamai, A., Okajima, E., and Kitamura, H. (1969) Histogenesis of urinary bladder tumors induced by *N*-butyl-*N*-(4-hydroxybutyl)-nitrosamine in rats. *Gann* **60**, 401–410
30. Bonfanti, M., Magagnotti, C., Bonati, M., Fanelli, R., and Airoldi, L. (1988) Pharmacokinetic profile and metabolism of *N*-nitrosobutyl-(4-hydroxybutyl)amine in rats. *Cancer Res.* **48**, 3666–3669
31. Airoldi, L., Magagnotti, C., Bonfanti, M., and Fanelli, R. (1990) Alpha-oxidative metabolism of the bladder carcinogens N-nitrosobutyl(4-hydroxybutyl)-amine and N-nitrosobutyl(3-carboxypropyl)amine within the rat isolated bladder. *Carcinogenesis* **11**, 1437–1440
32. Hashimoto, Y. and Kitagawa, H.S. (1974) In vitro neoplastic transformation of epithelial cells of rat urinary bladder by nitrosamines. *Nature* **252**, 497–499
33. Mimura, J., Yamashita, K., Nakamura, K., Morita, M., Takagi, T.N., Nakao, K., Ema, M., Sogawa, K., Yasuda, M., Katsuki, M., and Fujii-Kuriyama, Y. (1997) Loss of teratogenic response to 2,3,7,8-tetrachlorodibenzo-p-dioxin (TCDD) in mice lacking the Ah (dioxin) receptor. *Genes Cells* **2**, 645–654
34. Adachi, J., Mori, Y., Matsui, S., Takigami, H., Fujino, J., Kitagawa, H., Miller, C.A. 3rd, Kato, T., Saeki, K., and Matsuda, T. (2001) Indirubin and indigo are potent aryl hydrocarbon receptor ligands present in human urine. *J. Biol. Chem.* **276**, 31475–31478
35. Buckley, D.B. and Klaassen, C.D. (2009) Induction of mouse UDP-glucuronosyltransferase mRNA expression in liver and intestine by activators of aryl-hydrocarbon receptor, constitutive androstane receptor, pregnane X receptor, peroxisome proliferator-activated receptor alpha, and nuclear factor erythroid 2-related factor 2. *Drug Metab. Dispos.* **37**, 847–856
36. Reisman, S.A., Yeager, R.L., Yamamoto, M., and Klaassen, C.D. (2009) Increased Nrf2 activation in livers from Keap1-knockdown mice increases expression of cytoprotective genes that detoxify electrophiles more than those that detoxify reactive oxygen species. *Toxicol. Sci.* **108**, 35–47
37. Pollenz, R.S. (2002) The mechanism of AH receptor protein down-regulation (degradation) and its impact on receptor-mediated gene regulation. *Chemic-Biol. Interact.* **141**, 41–61
38. Pollenz, R.S. (2007) Specific blockage of ligand-induced degradation of the Ah receptor by proteasome but not calpain inhibitors in cell culture lines from different species. *Biochem. Pharmacol.* **74**, 131–143
39. Salghetti, S.E., Muratani, M., Wijnen, H., Futcher, B., and Tansey, W.P. (2000) Functional overlap of sequences that activate transcription and signal ubiquitin-mediated proteolysis. *Proc. Natl Acad. Sci. USA* **97**, 3118–3123
40. Muratani, M., Kung, C., Shokat, K.M., and Tansey, W.P. (2005) The F box protein Dsg1/Mdm30 is a transcriptional coactivator that stimulates Gal4 turnover and cotranscriptional mRNA processing. *Cell* **120**, 887–899
41. Lipford, J.R., Smith, G.T., Chi, Y., and Deshaies, R.J. (2005) A putative stimulatory role for activator turnover in gene expression. *Nature* **438**, 113–116
42. Chen, S., Operana, T., Bonzo, J., Nguyen, N., and Turkey, R.H. (2005) ERK kinase inhibition stabilizes the aryl hydrocarbon receptor. *J. Biol. Chem.* **280**, 4350–4359

MOLECULAR AND CELLULAR BIOLOGY, Dec. 2009, p. 6391–6400 Vol. 29, No. 24
0270-7306/09/$12.00 doi:10.1128/MCB.00337-09

Hypersensitivity of Aryl Hydrocarbon Receptor-Deficient Mice to Lipopolysaccharide-Induced Septic Shock▽†

Hiroki Sekine,[1,5] Junsei Mimura,[1,5] Motohiko Oshima,[1,5] Hiromi Okawa,[1,5] Jun Kanno,[2] Katsuhide Igarashi,[2] Frank J. Gonzalez,[3] Togo Ikuta,[4] Kaname Kawajiri,[4] and Yoshiaki Fujii-Kuriyama[1,5]*

The Center for Tsukuba Advanced Research Alliance and Institute of Basic Medical Sciences, University of Tsukuba, 1-1-1 Tennoudai, Tsukuba 305-8577, Japan[1]; Division of Molecular Toxicology, National Institute of Health Sciences, 1-18-1 Kamiyoga, Setagaya-ku, Tokyo 158-8501, Japan[2]; Laboratory of Metabolism, Center for Cancer Research, National Cancer Institute, National Institutes of Health, Bethesda, Maryland 20892[3]; Research Institute for Clinical Oncology, Saitama Cancer Center, 818 Komuro, Ina-machi, Kitaadachi-gun, Saitama 362-0806, Japan[4]; and SORST, Japan Science and Technology Agency, 4-1-8 Honcho, Kawaguchi, 332-0012, Japan[5]

Received 16 March 2009/Returned for modification 2 May 2009/Accepted 11 September 2009

Aryl hydrocarbon receptor (AhR), a ligand-activated transcription factor, is known to mediate a wide variety of pharmacological and toxicological effects caused by polycyclic aromatic hydrocarbons. Recent studies have revealed that AhR is involved in the normal development and homeostasis of many organs. Here, we demonstrate that AhR knockout (AhR KO) mice are hypersensitive to lipopolysaccharide (LPS)-induced septic shock, mainly due to the dysfunction of their macrophages. In response to LPS, bone marrow-derived macrophages (BMDM) of AhR KO mice secreted an enhanced amount of interleukin-1β (IL-1β). Since the enhanced IL-1β secretion was suppressed by supplementing Plasminogen activator inhibitor-2 (Pai-2) expression through transduction with Pai-2-expressing adenoviruses, reduced Pai-2 expression could be a cause of the increased IL-1β secretion by AhR KO mouse BMDM. Analysis of gene expression revealed that AhR directly regulates the expression of Pai-2 through a mechanism involving NF-κB but not AhR nuclear translocator (Arnt), in an LPS-dependent manner. Together with the result that administration of the AhR ligand 3-methylcholanthrene partially protected mice with wild-type AhR from endotoxin-induced death, these results raise the possibility that an appropriate AhR ligand may be useful for treating patients with inflammatory disorders.

The aryl hydrocarbon receptor (AhR) is a member of the basic helix-loop-helix/Per-Arnt-Sim homology superfamily and is involved in the induction of drug-metabolizing enzymes and the susceptibility of cells to a variety of cytotoxicities induced by dioxins (9). AhR is a ligand-activated transcription factor activated by polycyclic aromatic hydrocarbons (PAHs), such as 3-methylcholanthrene (3MC) and 2′,3′,7′,8′-tetrachlorodibenzo-*p*-dioxin (TCDD). Under normal conditions, AhR exists in the cytoplasm in a complex with Hsp90, XAP2, and p23 (22). After binding a ligand, AhR translocates into the nucleus where it dimerizes with its partner molecule, AhR nuclear translocator (Arnt), and acts as a transcriptional activator to regulate the expression of target genes, such as those expressing drug-metabolizing cytochrome P450 (Cyp1a1, 1a2, and 1b1) and NAD(P)H: quinone oxidoreductase (Nqo), by binding to xenobiotic response element (XRE) sequences in their promoter regions (9). By using AhR knockout (AhR KO) mice, it has been demonstrated that AhR is essential not only for the induction of drug-metabolizing enzymes but also for most, if not all, of the toxicological effects caused by TCDD, including immunosuppression, thymic atrophy, teratogenesis, and hyperplasia (6, 7, 17, 24), the mechanisms for which are largely unknown. Recently, careful investigation into the loss of functions in AhR KO mice has also revealed that AhR is involved in the normal development of several organs, including the liver, heart, vascular tissues, and reproductive organs (1, 2, 6, 8, 15, 24). In addition, AhR has been found to play a key role in the differentiation of regulatory T cells Treg, Th17, and Th1 from naive CD4 T cells by regulating their expression of Foxp3 or by as-yet-unknown mechanisms (14, 20, 23, 32). From these studies, one of the general features of AhR that begins to emerge is that it serves as a multifunctional regulator in a large number of areas, ranging from drug metabolism to innate immunity for protection against invasive xenobiotics. In the work presented here, we demonstrated that AhR KO mice were hypersensitive to lipopolysaccharide (LPS)-induced septic shock, mainly due to the dysfunction of their macrophages. AhR KO mouse macrophages secreted an enhanced amount of interleukin-1β (IL-1β) in response to LPS treatment and had markedly reduced Plasminogen activator inhibitor-2 (Pai-2) mRNA concentrations, as revealed by DNA microarray analysis. Pai-2 was reported to be a negative regulator of IL-1β secretion through its inhibition of caspase-1 (10), suggesting that the enhanced secretion of IL-1β by AhR KO macrophages in response to LPS may have been due to the reduced level of Pai-2. We showed that AhR directly regulates the expression of inhibitory Pai-2, in an LPS-dependent manner, through a mechanism involving NF-κB but not Arnt.

* Corresponding author. Present address: 5-18-7 Honkomagome, Bunkyo-ku, Tokyo 113-0021, Japan. Phone and fax: 3-3941-2200. E-mail: y.k_fujii@nifty.com.

† Supplemental material for this article may be found at http://mcb.asm.org/.

▽ Published ahead of print on 12 October 2009.

MATERIALS AND METHODS

Mice. AhR knockout (AhR KO) mice were generated as described previously (17). These mice were back-crossed with C57BL/6J mice at least 10 times. Age-matched mice (10 weeks) were intraperitoneally injected with 20 mg of

LPS/kg of body weight. Mice with floxed *Arnt* (30) and *AhR* (Jackson laboratory) alleles were crossed to LysM Cre mice to specifically delete these genes in their macrophages. $AhR^{flox/-}$ and $AhR^{flox/-}$::LysM Cre mice were generated by mating $AhR^{flox/flox}$::LysM Cre and $AhR^{-/-}$ (AhR KO) mice. These age-matched mice (9 to 11 weeks old) were intraperitoneally injected with 25 mg LPS/kg. Mouse survival was checked every 6 or 12 h. 3MC (Wako, Osaka) at 10 μl (4 mg/ml 3MC)/g of body weight or 10 μl corn oil/g was intraperitoneally injected. After 2 h, each mouse was intraperitoneally injected with 30 mg LPS/kg. LPS (from *Escherichia coli* 0111:B4) was purchased from Sigma.

Preparation of macrophages. Bone marrow cells were obtained from the femurs of 8- to 12-week-old mice. The bone marrow-derived macrophages (BMDM) used for each experiment were isolated by culturing bone marrow cells in the presence of 10 ng/ml granulocyte-macrophage colony-stimulating factor (PeproTech) for 7 days and washing the attached cells with phosphate-buffered saline (PBS) three times. For cytokine assays, washed cells were collected with a scraper, plated at 2×10^6 cells/ml in 96-well plates, and cultured with 10 ng/ml LPS for 8 h.

For isolation of peritoneal exudate macrophages (PEMs), mice were intraperitoneally injected with 2 ml of 4% thioglycolate. Peritoneal cells were isolated from exudates of the peritoneal cavity 3 days after injection, incubated for 3 h in appropriate plates, and washed with PBS. The adherent cells were used for experiments.

Measurement of cytokines. Mice were intraperitoneally injected with 20 mg/kg LPS and bled 2 h after injection. Plasma concentrations of IL-1β, tumor necrosis factor alpha (TNF-α), IL-6, gamma interferon (IFN-γ), IL-12, and IL-18 were determined by enzyme-linked immunosorbent assay (ELISA) (Biosource). BMDM of mice with wild-type AhR (AhR WT mice) and AhR KO at 2×10^6 cells/ml were incubated with 10 ng/ml LPS for 8 h, and their culture supernatants were assessed for cytokines using mouse TNF-α and IL-1β ELISAs (Biosource).

Cell culture. All cells were maintained in RPMI medium (Sigma) supplemented with 10% fetal bovine serum (HyClone) and penicillin/streptomycin (Gibco) under 5.0% CO_2 at 37°C.

Caspase inhibitors. BMDM of AhR KO mice at 2×10^6 cells/ml were incubated with dimethyl sulfoxide (DMSO) or 80 μM Z-YVAD-FMK (caspase-1 inhibitor VI; Merck) or 100 μM Z-VAD-FMK (caspase inhibitor VI; Merck) for 30 min before LPS (10 ng/ml) stimulation. The BMDM were incubated for 8 h, and their culture supernatants were assessed for cytokines using a mouse IL-1β ELISA (Biosource).

Virus infections. Adenoviruses expressing green fluorescent protein (GFP), human Pai-2 (hPai-2), and human Bcl-2 (hBcl-2) were purchased from Vector Biolabs (Philadelphia). BMDM from AhR KO mice were infected for 12 h with adenoviruses expressing GFP, hPai-2, and hBcl-2 at a multiplicity of infection of 100. Infected BMDM were washed with PBS, followed by 12 h of incubation. As it was reported that adenoviral vectors enhanced IL-1β secretion in macrophages (19), IL-1β levels were investigated in these incubation supernatants by ELISA. At this point, no IL-1β was observed in the supernatants. Therefore, the cells were washed, collected with a scraper, and plated at 2×10^6 cells/ml in 96-well plates. The cells were treated with 10 ng/ml of LPS for an additional 8 h.

Retroviral infection was performed as follofws: pQC-mAhR, a cloned murine AhR (mAhR) fragment in pQCXIN (Clontech), and pQCXLN for LacZ expression (as a control) were transfected into PT67 cells that were then cultured for 24 h. The culture medium was replaced with fresh medium, and the culture was continued for an additional 24 h. This culture medium was used as the retrovirus particle source.

Microarray analysis. Total RNA samples were purified using Isogen before being processed and hybridized to Affymetrix mouse genome 430 2.0 arrays (Affymetrix). The experimental procedures for the GeneChip analyses were performed according to the Affymetrix technical manual.

Generation of stable transformant cell lines. ANA-1 cells were the kind gift of L. Varesio (3). ANA-1 cells were transduced with LacZ- or AhR-expressing retroviruses in a suspension with 8 mg/ml of Polybrene. One day after infection, the infected cells were replated and incubated in a selection medium containing 0.5 mg/ml of Geneticin (Gibco).

Plasmids. pcDNA3-p65 and pcDNA3-AhR were generated by inserting AhR and p65 cDNA fragments, excised from pBS-mAhR and pBS-mp65 (murine p65), into the pcDNA3 vector. The 2.7-kb fragment upstream of the Pai-2 transcription start site was generated by PCR (primers 5′-gaagcttGGGTTGCA GATCCCTTTAGC-3′ and 5′-ccatggtggCTGACACACAGGAAATGCTTC-3′; lowercase indicates restriction site sequences for cloning), using a BAC vector carrying the Pai-2 gene as a template, and then cloned into the pBS vector. After sequencing, the construct was cleaved with HindIII/NcoI, and the isolated insert was cloned into the HindIII/NcoI-digested pGL4.10 (Promega) to produce pGL4-Pai-2 (−2.7 kb). The 0.8-kb fragment upstream of the Pai-2 transcription start site was generated by PCR (primers 5′-ggaattcGAGAAGTGATCTGGTA GATG-3′ and 5′-ccatggtggCTGACACACAGGAAATGCTTC-3′) using pGL4-Pai-2 (−2.7 kb) as a template and cloned into the pBS vector. After sequencing, the construct was cleaved with HindIII/NcoI, and the isolated insert was cloned into the HindIII/NcoI-digested pGL4.10 (Promega) to produce pGL4-Pai-2 (−0.8 kb). pGL4-Pai-2 (−0.55 kb) was produced by cleaving pGL4-Pai-2 (−2.7 kb) with NdeI/EcoRV. pGL4-Pai-2 (−0.1 kb) was generated in a similar manner, using primers 5′-GATGTCTTTATGAGTAAAATGTTGAATCA-3′ and 5′-cca tggtggCTGACACACAGGAAATGCTTC-3′. pGL4-Pai-2 (−0.55 kb C/EBPβ mutant) was generated by site-directed mutagenesis using a Sculptor in vitro mutagenesis system (Amersham) with pGL4-Pai-2 (−0.55 kb) as a template and primer pair 5′-GATTTAAAATTGGAAAggGCTAAATTCTTGAATTTTGAA TGACATCAC-3′ and 5′-GTGATGTCATTCAAAATTCAAGAATTTAGCcc TTTCCAATTTTAAATC-3′.

RNA preparation and reverse transcription PCR (RT-PCR). Total RNA was prepared using Isogen (Nippon Gene, Tokyo) according to the manufacturer's protocol. cDNA synthesis from 1 μg of total RNA was carried out using Super-Script II reverse transcriptase (Invitrogen, United States). Real-time PCR was performed using an ABI7300 real-time PCR system (Applied Biosystems) and Platinum SYBR green quantitative PCR SuperMix (Invitrogen, United States). Each sample was normalized to the expression of β-actin as a control. The primer sequences were as follows: Pai-2, 5′-GCATCCACTGGCTTGGAA-3′ and 5′-GGGAATGTAGACCACAACATCAT-3′; Bcl-2, 5′-GTGGTGGAGGA ACTCTTCAGGGATG-3′ and 5′-GGTCTTCAGAGACAGCCAGGAGAAAT C-3′; AhR, 5′-TTCTATGCTTCCTCCACTATCCA-3′ and 5′-GGCTTCGTCC ACTCCTTGT-3′; Arnt, 5′-GGACGGTGCCATCTCGAC-3′ and 5′-CATCTG GTCATCATCGCATC-3′; Mmp-8, 5′-CCACACACAGCTTGCCAATGCC T-3′ and 5′-GGTCAGGTTAGTGTGTGTCCACT-3′; Nqo1, 5′-TTTAGGGTC GTCTTGGCAAC-3′ and 5′-AGTACAATCAGGGCTCTTCTCG-3′; AhR repressor, 5′-CCTGTCCCGGGATCAAAGATG-3′ and 5′-CTCACCACCAG AGCGAAGCCATTGA-3′; IL-1β, 5′-CTGAAGCAGCTATGGCAACT-3′ and 5′-GGATGCTCTCATCTGGACAG-3′; TNF-α, 5′-CTGTAGCCCACGTCGT AGC-3′ and 5′-TTGAGATCCATGCCGTTG-3′; Cox-2, 5′-GCATTCTTTGCC CAGCACTT-3′ and 5′-AGACCAGGCACCAGACCAAAG-3′; β-actin, 5′-GA CAGGATGCAGAAGGAGAT-3′ and 5′-TTGCTGATCCACATCTGCTG-3′; hPai-2, 5′-CCCAGAACCTCTTCCTCTCC-3′ and 5′-CATTGGCTCCCACTT CATTA-3′; and hBcl-2, 5′-GTGTGTGGAGAGCGTCAACC-3′ and 5′-GAGA CAGCCAGGAGAAATCAAA-3′.

Reporter assays. All luciferase assays were performed using a dual-luciferase reporter assay system according to the manufacturer's protocol (Promega), with some modifications. RAW 264.7 cells (2.0×10^4 cells/well) were plated in 24-well plates 24 h prior to transfection. Cells were cotransfected with 100 ng pGL4-Pai-2 (various lengths in kilobases) (see "Plasmids"), 1 ng *Renilla* luciferase (as an internal control), and 1 ng pcDNA3-p65 and/or pcDNA3-AhR using Fu-GENE HD transfection reagent (Roche) according to the manufacturer's protocol. All cells were incubated for 12 h at 37°C after transfection, treated with 10 ng/ml LPS, and incubated for an additional 6 h.

Co-IP assays. AhR WT PEMs or transfected 293T cells were washed with ice-cold PBS, followed by buffer containing 20 mM HEPES, pH 7.4, 125 mM NaCl, 1% Triton X-100, 10 mM EDTA, 2 mM EGTA, 2 mM Na_3VO_4, 50 mM sodium fluoride, 20 mM $ZnCl_2$, 10 mM sodium pyrophosphate (31). The cells were harvested by scraping, centrifuged at 5,000 rpm at 4°C for 5 min, and suspended in immunoprecipitation (IP) buffer containing a protease inhibitor cocktail (Roche). The cells were vortexed and placed on ice for 10 min. The samples were then centrifuged at 15,000 rpm for 5 min at 4°C, and the supernatants were saved as whole-cell lysates.

The prepared whole-cell lysate (250 μl) was incubated with anti-immunoglobulin G, anti-AhR antibody, or anti-p65 for 2 h at 4°C. The reaction mixture was supplemented with 20 μl of protein A-agarose beads (Amersham). After being incubated for an additional 1 h at 4°C, the beads were washed three times with IP buffer containing protease inhibitor cocktail and resuspended in sodium dodecyl sulfate (SDS) sample buffer. The coimmunoprecipitated proteins were resolved by SDS-polyacrylamide gel electrophoresis (PAGE), and Western blot analysis was performed.

ChIP assays. Chromatin IP (ChIP) assays were performed with PEMs from AhR WT and AhR KO mice. PEMs were stimulated with 10 ng/ml LPS for 60 min and then fixed with formaldehyde for 10 min. The cells were lysed and sheared by sonication. The lysis solution was incubated with immunoglobulin G or preimmune serum and protein A-agarose for 2 h to remove nonspecific DNA binding. The solution was incubated overnight with a specific antibody, followed by incubation with protein A-agarose saturated with salmon sperm DNA. Precipitated DNA was analyzed by real-time PCR using primer pair 5′-GGAAGT TCCCTGAGGCTTATAGG-3′ and 5′-ATGGAAGCACATACATAAGAACA

TGG-3′ for the NF-κB binding site of Pai-2, 5′-TGAGTGTGAGTGGTGCAG ATTAC-3′ and 5′-CCTCCCACACAGCTCTTTTTTC-3′ for mPai-2 TATA, 5′-CGGAGGGTAGTTCCATGAAA-3′ and 5′-CAGGCTTTTACCCACGCAA A-3′ for the NF-κB binding site of mCox2, and 5′-CGCAACTCACTGAAGC AGAG-3′ and 5′-TCCTTCGTGAGCAGAGTCCT-3′ for mCox-2 TATA. The antibodies used were as follows: anti-AhR serum, preimmune serum, anti-p65, and anti-PolII antibodies (Santa Cruz).

Western blot analyses. Cells were dissolved in SDS sample buffer, and proteins were separated by SDS-PAGE for Western blot analysis. The proteins were then transferred to polyvinylidene difluoride membranes and blocked in 3% skim milk for 30 min. Each antibody was used as a primary reagent, and after being washed three times with Tris-borate-EDTA containing 0.1% Triton X-100, membranes were incubated with species-specific horseradish peroxidase-conjugated secondary antibody (Zymed). The protein-antibody complexes were visualized by using an enhanced chemiluminescence detection system (Amersham) according to the manufacturer's recommendations. Nuclear extracts were prepared by a standard method (25). The antibodies used were as follows: anti-Arnt serum (28); anti-AhR (Biomol); anti-Pai-2, anti-p65, and antilamin antibodies (Santa Cruz); and antitubulin antibody (Sigma).

RESULTS

High susceptibility of AhR-deficient mice to LPS-induced endotoxin shock. To investigate the function of AhR in acute inflammation in vivo, we performed studies of experimental LPS-induced endotoxin shock. For these studies, 10-week-old AhR WT and AhR KO mice were injected intraperitoneally with 20 mg/kg LPS. After 24 h, while all of the AhR WT mice survived, most of the AhR KO mice (80%) had died (Fig. 1A). These data indicate that AhR-deficient mice were highly susceptible to LPS-induced endotoxin shock. To explain the increased sensitivity of AhR KO mice to septic shock, the plasma concentrations of several inflammatory cytokines were measured 2 h after LPS challenge. Consistent with the enhanced susceptibility of AhR KO mice to the LPS treatment, AhR KO mice had marked increases in plasma IL-1β, IL-18, and TNF-α levels ($P < 0.001$), with modest increases in IL-6 and IFN-γ (Fig. 1B). In contrast, there was no difference in plasma IL-12p70 levels (Fig. 1B). Administration of 3MC, an AhR ligand, before LPS treatment (30 mg/kg) made the AhR WT mice significantly more resistant to septic shock than the mice that were not treated with 3MC ($P = 0.002$) (Fig. 1C). Together with the fact that there was essentially no effect of 3MC on AhR KO mice, these results suggested that activated AhR could play an anti-inflammatory role.

Increased susceptibility of mice with AhR KO macrophages to LPS-induced endotoxin shock. Since macrophages play an important role in sensitivity to LPS toxicity, we generated mice with macrophages deficient in AhR ($AhR^{flox/-}$::LysM Cre [ΔAhR Mac] mice) to evaluate the contribution of macrophages to the LPS hypersensitivity of AhR KO mice. When ΔAhR Mac and control mice ($AhR^{flox/-}$) were injected intraperitoneally with 25 mg/kg LPS, most of the ΔAhR Mac mice (80%) had died at 48 h after LPS challenge, while 60% of the control mice survived ($P = 0.03$) (Fig. 2A). Together with the previous results, these data showed that dysfunctional AhR-deficient macrophages are one of the main causes of LPS hypersensitivity in AhR KO mice.

Elevated IL-1β secretion from AhR KO BMDM in response to LPS. To further investigate the cause of the aberrant cytokine secretion by LPS-challenged AhR KO mice, we next asked if there were any differences in the production of proinflammatory cytokines by AhR WT and AhR KO mouse

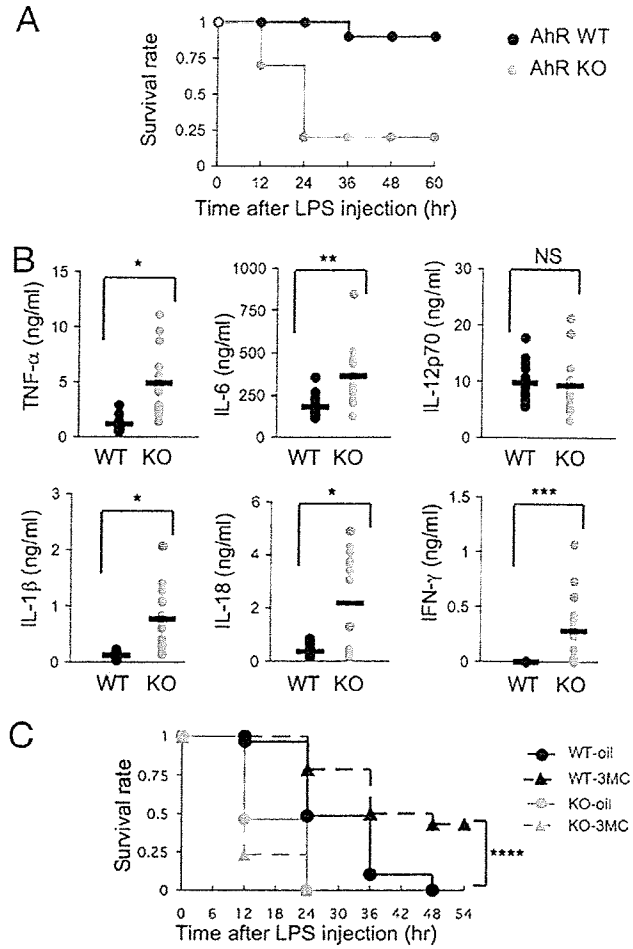

FIG. 1. High susceptibility of AhR KO mice to LPS-induced endotoxin shock. (A) Survival of AhR WT and AhR KO mice ($n = 10$) after LPS challenge (20 mg/ml). (B) TNF-α, IL-6, IL-12p70, IL-1β, IL-18, and IFN-γ plasma levels 2 h after LPS challenge (20 mg/ml). Horizontal bars show the mean results. (C) Partial protection of AhR WT mice from septic shock by intraperitoneal injection of 3MC at 2 h before LPS challenge (30 mg/ml) and survival of corn oil-injected mice. AhR WT-oil, $n = 29$; AhR WT-3MC, $n = 28$; AhR KO-oil, $n = 13$; AhR KO-3MC, $n = 13$. *, $P < 0.001$; **, $P = 0.001$; ***, $P < 0.005$; ****, $P = 0.002$; NS, not significant.

BMDM in response to LPS stimulation. Macrophages from the bone marrow of AhR WT and AhR KO mice were challenged with 10 ng/ml LPS for 8 h, and then the levels of TNF-α and IL-1β in the culture medium were assessed by ELISA. Compared to the levels in AhR WT BMDM, the levels of IL-1β secretion by AhR KO BMDM were markedly elevated, along with slight increases in TNF-α, in response to LPS treatment ($P < 0.001$) (Fig. 2B, left). However, IL-1β mRNA levels were not altered between AhR WT and AhR KO BMDM (Fig. 2C, left). These data indicated that AhR deficiency markedly increased IL-1β accumulation due to its enhanced secretion rather than its increased synthesis.

Expression of AhR-dependent genes in macrophages. We next performed microarray analysis of AhR WT and AhR KO mouse macrophages to comprehensively investigate the AhR-

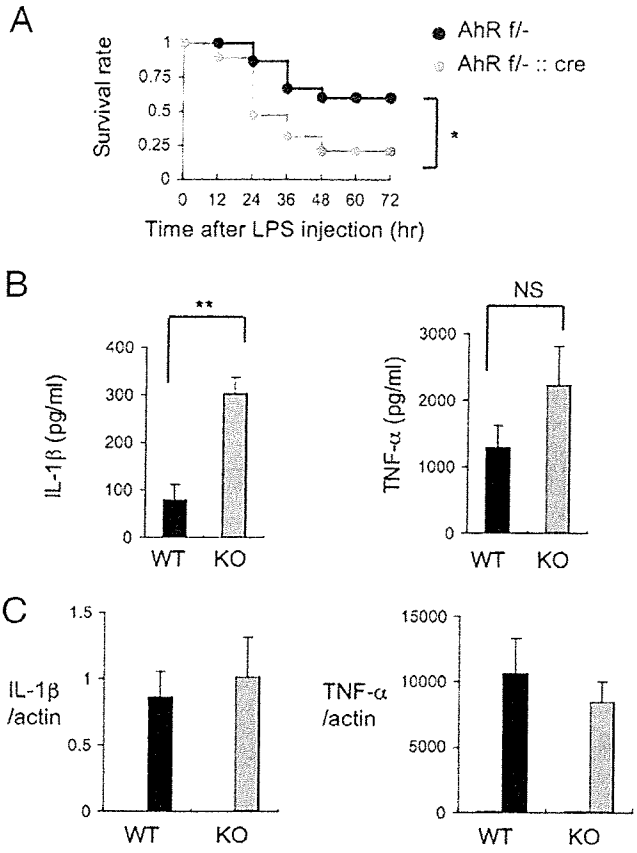

FIG. 2. LPS induces abnormal secretion of IL-1β by BMDM from AhR KO mice. (A) Survival of $AhR^{flox/-}$ (AhR f/−; $n = 15$) and $AhR^{flox/-}$::LysM Cre (AhR f/−::cre; $n = 19$) mice after LPS challenge (25 mg/ml). (B) IL-1β and TNF-α levels in the culture supernatants of AhR WT and AhR KO BMDM 8 h after LPS stimulation (10 ng/ml) ($n = 4$). (C) Relative expression levels of IL-1β and TNF-α mRNA 4 h after LPS stimulation (10 ng/ml) of AhR WT and AhR KO BMDM. Gray and black bars show results with LPS; white bars show results for untreated cells. Error bars show standard deviations. *, $P = 0.03$; **, $P < 0.001$; NS, not significant.

dependent changes in gene expression that were related to IL-1β secretion (Table 1). Among the genes whose expression was reduced in AhR KO macrophages, we noted the markedly reduced levels of expression of the Pai-2 and Bcl-2 genes. These genes were significant because they had been reported to negatively regulate IL-1β secretion by inhibiting the activity of caspase-1 (5, 10). Consistent with the notion that the enhanced secretion of IL-1β is due to the activation of caspase-1, treatment with the caspase inhibitors Z-YVAD-FMK and Z-VAD-FMK markedly reduced the secretion of IL-1β in AhR KO BMDM (Fig. 3A). To confirm their reduced expression in AhR KO BMDM, Pai-2 and Bcl-2 mRNA expression levels were determined by real-time RT-PCR in AhR WT and AhR KO BMDM (Fig. 3B). Figure 3B shows that Pai-2 and Bcl-2 mRNA expression levels were clearly reduced in AhR KO BMDM. To investigate whether the increased IL-1β secretion in AhR KO BMDM was due to their reduced Pai-2 and Bcl-2 expression, the expression of these proteins was supplemented in AhR KO BMDM by infection with adenoviral vectors expressing hPai-2 and hBcl-2 (Fig. 3D). The efficiency of the adenoviral gene transfer, as monitored by the expression of GFP, was estimated to be >90% (data not shown). Compared with control adenoviral expression of GFP, transfer of the hPai-2 gene into AhR KO BMDM significantly inhibited LPS-induced secretion of IL-1β (Fig. 3C), but almost no effect was observed with Bcl-2 expression. Bcl-2 has been reported to suppress IL-1β secretion that is specifically processed through the NALP1 complex and regulated by muramyl dipeptide, which is usually a contaminant in commercial LPS (5). These results suggested that the enhanced IL-1β secretion in response to LPS was due not to processing through the NALP1 complex (5) but to processing through the NALP3 complex, an inflammasome-containing caspase-1 regulated by LPS (16), and that decreased Pai-2 expression is at least one of the causes for the increased IL-1β secretion by AhR KO BMDM after LPS treatment.

Arnt is not required for enhancement of LPS-induced Pai-2 expression by AhR. It has been reported that LPS stimulation induces Pai-2 expression (21, 26). Figure 4A and B show that the induction of both Pai-2 mRNA and protein expression was remarkably reduced in AhR KO macrophages compared with the levels in AhR WT macrophages. Interestingly, AhR mRNA and protein expression levels were also induced by LPS stimulation (Fig. 4A and B). In response to various PAHs, AhR is known to act, in most cases, as a transcriptional activator, in heterodimer formation with Arnt. Although the mouse Pai-2 promoter does not have any obvious XRE sequences (GCGTG) in its regions 5 kb upstream and down-

TABLE 1. Decreased gene expression in AhR KO PEMs revealed by cDNA microarray analysis

Fold change	Value for		Gene name	Gene product
	WT PEMs	KO PEMs		
14.0	0.561	0.040	*Gsta3*	Glutathione *S*-transferase alpha 3
10.2	7.826	0.767	*Pai-2*	Plasminogen activator inhibitor-2
5.5	9.354	1.700	*Cyp1b1*	Cytochrome P450, family 1, subfamily b, polypeptide 1
4.6	0.206	0.045	*Nkrf*	NF-κB repressing factor
3.6	1.922	0.541	*Cxcl5*	Chemokine (C-X-C motif) ligand 5
3.1	13.670	4.444	*Mmp8*	Matrix metallopeptidase 8
2.9	1.406	0.489	*Cxcl13*	Chemokine (C-X-C motif) ligand 13
2.6	2.111	0.800	*Lrrc27*	Leucine-rich repeat-containing 27
2.5	3.466434	1.394728	*Ctgf*	Connective tissue growth factor
2.2	3.849141	1.722473	*Mcoln3*	Mucolipin 3
2.2	1.204793	0.550093	*Nqo1*	NAD(P)H dehydrogenase, quinone 1
2.0	6.96623	3.453017	*Ier3*	Immediate early response 3
2.0	0.596479	0.294062	*Bcl2*	B-cell leukemia/lymphoma 2

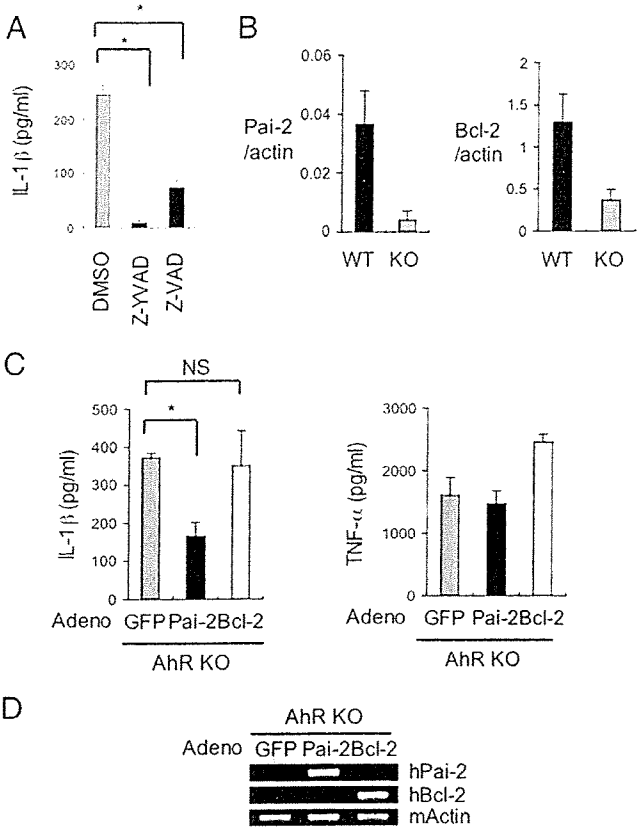

FIG. 3. Decreased Pai-2 expression is one of the causes of the increased IL-1β secretion by LPS-treated AhR KO BMDM. (A) Inhibition of IL-1β oversecretion from AhR KO BMDM by treatment with caspase-1 inhibitor (Z-YVAD-FMK) or caspase inhibitor (Z-VAD-FMK). (B) Relative expression levels of Pai-2 and Bcl-2 mRNA in AhR WT and AhR KO BMDM. (C) The effect of hPai-2 and hBcl-2 reconstitution on the LPS-induced secretion of IL-1β and TNF-α by AhR KO BMDM. BMDM from AhR KO mice were infected with the individual adenovirus (adeno) vectors and then washed and incubated for 24 h. IL-1β and TNF-α levels in the supernatants 8 h after LPS stimulation ($n = 3$) were determined by ELISA. (D) Assessment of hPai-2 and hBcl-2 mRNA expression in adenovirus (adeno) vector-infected BMDM by conventional RT-PCR. Error bars show standard deviations. *, $P < 0.001$; NS, not significant.

stream of the transcription start site, we were interested in determining whether Arnt was also involved in the inducible expression of Pai-2 by LPS. Other AhR target genes identified by the microarray analysis, e.g., the matrix metalloproteinase (Mmp-8) gene and the NAD(P)H:quinone oxidoreductase 1 (Nqo1) gene (Table 1), have characteristic XRE sequences in their promoter regions and were also induced by 3MC. As expected, the induction of their expression was greatly reduced in Arnt KO and Arnt small interfering RNA (siRNA)-treated macrophages (Fig. 4E; also see Fig. S1 in the supplemental material). In stark contrast, the expression of Pai-2 was not much different in Arnt KO and Arnt siRNA-treated macrophages, indicating that Arnt is not involved in regulating Pai-2 gene expression (Fig. 4D; also see Fig. S1 in the supplemental material) and that AhR regulates Pai-2 gene expression by a noncanonical mechanism. Consistent with these observations, macrophage-specific conditional deletion of Arnt did not significantly alter the sensitivity to LPS treatment (Fig. 4F).

DNA elements regulating Pai-2 gene expression. We were interested in further investigating how AhR regulates Pai-2 gene expression in macrophages. It has been previously reported that LPS-induced Pai-2 expression requires NF-κB activation (21) and that AhR and p65 physically interact with each other (31). With those results in mind, we constructed a reporter gene by fusing a 2.7-kb sequence upstream of the mouse Pai-2 transcription start site to the luciferase gene (see Fig. S2 in the supplemental material). This 2.7-kb Pai-2 reporter gene contained a previously reported NF-κB site (21). When the AhR expression vector alone was transfected into RAW 264.7 cells, it did not enhance LPS-induced reporter gene expression. In contrast, cotransfection of both AhR and p65 did (Fig. 5A). To identify the sequence responsible for enhancing the LPS-induced activation of the reporter gene, we constructed an 0.8-kb Pai-2 reporter gene by deleting the sequence from −2.7 to −0.8 kb, which contained the previously reported NF-κB site (see Fig. S2 in the supplemental material). With this 0.8-kb Pai-2 construct, the addition of AhR and p65 no longer enhanced the activity in response to LPS treatment (Fig. 5A), indicating that the sequence between −0.8 and −2.7 kb, containing an NF-κB site, is responsible for enhancing Pai-2 gene activation in response to AhR and NF-κB. Further downstream, we noticed the presence of a putative C/EBPβ binding sequence (around 250 base pairs upstream of the transcription initiation site), which has been reported to be responsible for LPS-induced activation of the gene (4). Deletion or point mutation of this sequence was found to abrogate the ability of LPS to induce this gene, indicating that this C/EBPβ binding site functions as an enhancer sequence in the LPS response (see Fig. S2 in the supplemental material).

Recruitment of transcription factors necessary for LPS-induced Pai-2 expression. When macrophages were treated with LPS, p65 translocated from the cytoplasm into the nucleus independently of AhR (Fig. 5B), as reported previously. However, without AhR, ChIP revealed that p65 was not recruited to the enhancer sequence in the Pai-2 gene, which contains an NF-κB site (Fig. 5E). In WT macrophages, nuclear-translocated p65 was only recruited to the enhancer sequence of the Pai-2 gene together with AhR. PolII was concomitantly recruited to the TATA sequence of the Pai-2 gene in AhR WT but not AhR KO macrophages. Surprisingly, we observed that LPS induced AhR binding to the Pai-2 NF-κB site, as shown by ChIP using an anti-AhR antiserum. Co-IP assays revealed that AhR and p65 interacted in macrophages (Fig. 5C), consistent with a previous report (31). On the other hand, expression of the Cox-2 gene is known to be activated by LPS through recruitment of p65 to its NF-κB binding site, and this occurs independent of AhR (Fig. 5D), with concomitant binding of PolII to the transcription initiation site (TATA) of the Cox-2 gene (Fig. 5E). Arnt was not recruited to the Pai-2 promoter by ChIP assay (data not shown), consistent with normal Pai-2 expression in the macrophages from $Arnt^{flox/-}$::LysM Cre mice (Fig. 4D).

As shown in Fig. S3 in the supplemental material, the CCAAT box sequence in the Pai-2 gene was recognized by C/EBPβ in an LPS-dependent manner in both AhR WT and KO macrophages. This binding of C/EBPβ to the Pai-2 pro-

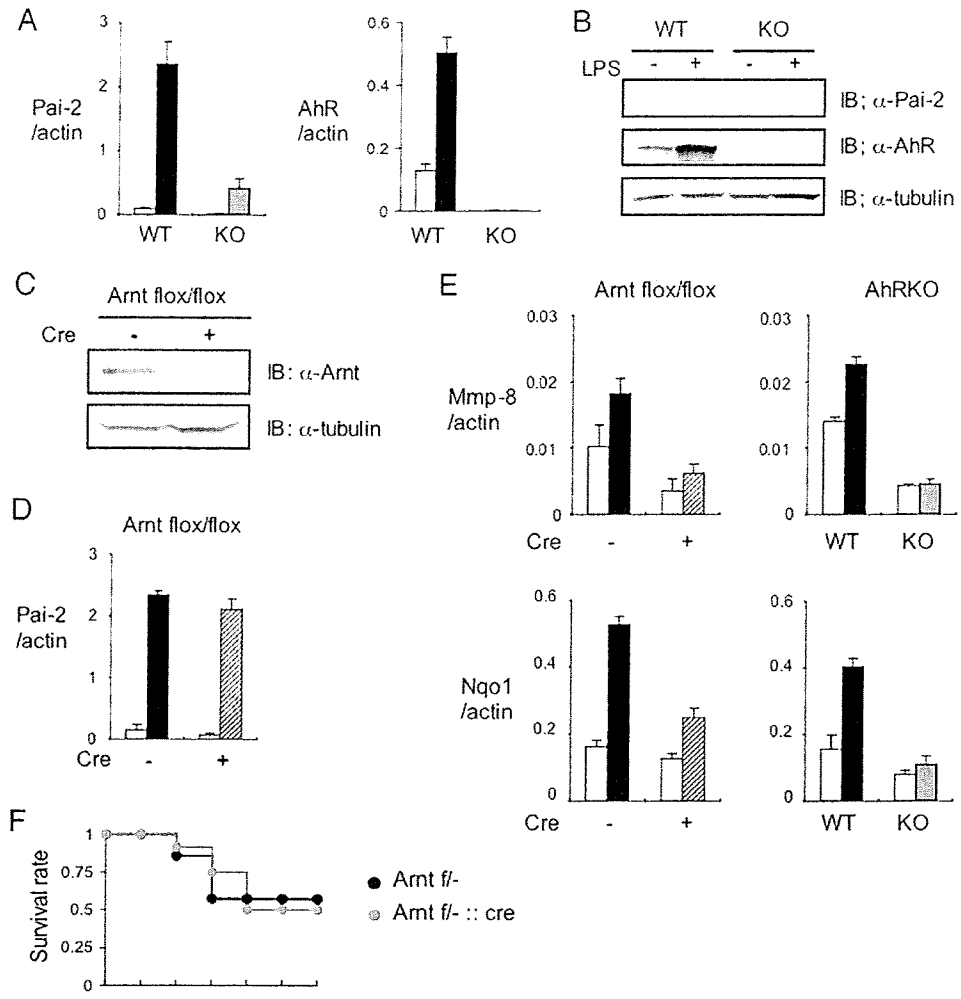

FIG. 4. Arnt is not required for LPS-induced enhancement of Pai-2 expression. (A) Relative Pai-2 and AhR mRNA expression levels in AhR WT and AhR KO PEMs 4 h after treatment with (black or gray bars) or without (white bars) LPS (10 ng/ml). (B) Immunoblot analysis of Pai-2 and AhR expression in AhR WT and KO PEMs after a 16-h incubation with LPS (10 ng/ml). (C) Immunoblot analysis of Arnt in $Arnt^{flox/flox}$ and $Arnt^{flox/flox}$::LysM Cre PEMs. (D) Relative Pai-2 mRNA expression levels 4 h after incubation of $Arnt^{flox/flox}$ (black bar) and $Arnt^{flox/flox}$::LysM Cre (hatched bar) PEMs with LPS (10 ng/ml). (E) Left, relative expression levels of Mmp-8 and Nqo1 mRNA in $Arnt^{flox/flox}$ (black bar) and $Arnt^{flox/flox}$::LysM Cre (hatched bar) PEMs treated with DMSO (white bars) or 3MC (black or hatched bar) (1 μM). Right, relative expression levels of Mmp-8 and Nqo1 mRNA in AhR WT (black bar) and AhR KO (gray bar) PEMs treated with DMSO (white bars) or 3MC (black or gray bar) (1 μM). (F) Survival of $Arnt^{flox/-}$ (Arnt f/−; n = 7) and $Arnt^{flox/-}$::LysM Cre (Arnt f/−::cre; n = 12) mice after LPS challenge (25 mg/ml). Error bars show standard deviations. IB, immunoblot; +, present; −, absent; α, anti.

moter might explain the weak LPS-induced activation of Pai-2 gene expression in AhR KO macrophages (Fig. 4A; also see Fig. S3 in the supplemental material), as described in the previous section.

The requirement of the functional domains of AhR for AhR-dependent Pai-2 expression. To determine the functional domains of AhR for AhR-dependent Pai-2 expression, we investigated the Pai-2 expression in ANA-1 cells, which were transfected with various AhR mutants (Fig. 6). Compared with the levels in ANA-1 cells transfected with full-length AhR, we observed much lower levels of expression of Pai-2 in the ANA-1 cells transfected with AhR NLSm (a mutant located predominantly in the cytoplasm) (Fig. 6B, bars 3, 4, 11, and 12). On the other hand, transfection with AhR CA (a constitutively active mutant located predominantly in the nucleus) gave a result for Pai-2 expression comparable to that of the transfection with full-length AhR (Fig. 6B, bars 3, 4, 7, and 8). These results indicated that nuclear AhR functions in AhR-dependent Pai-2 expression. The fractionation of AhR indicated that a small but significant amount of AhR existed in the nucleus without treatment with ligands such as 3MC, in contrast with the large amount in the cytoplasm (Fig. 5B), consistent with the previous report that AhR has functional nuclear localization signal and nuclear export signal sequences and shuttles between the cytoplasm and nucleus. It is reported that when nuclear export is inhibited by trichomycin B or phosphorylation at S68, AhR accumulates in the nucleus (12). Therefore, it could be considered that in macrophages, AhR is in-

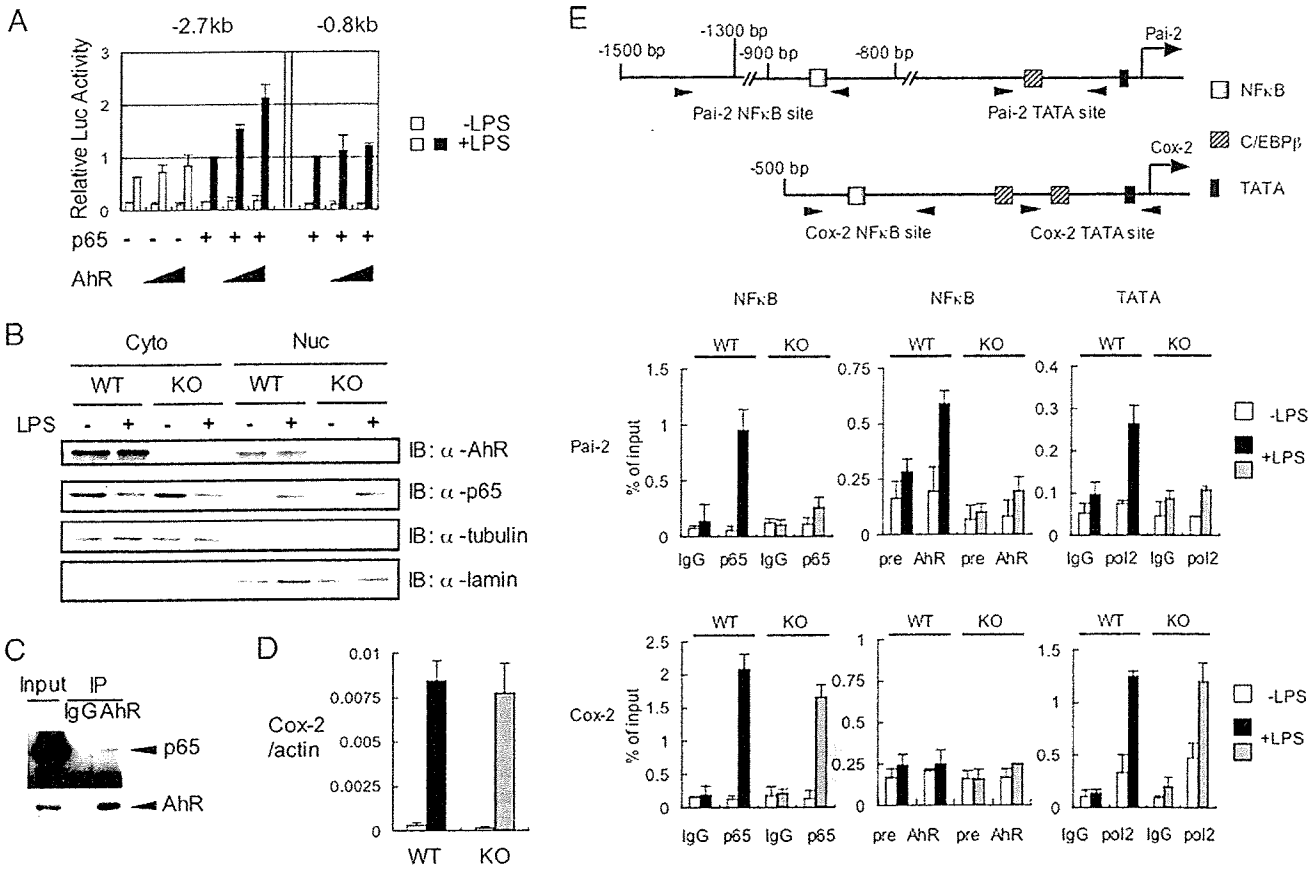

FIG. 5. Recruitment of transcription factors necessary for LPS-induced Pai-2 expression. (A) LPS-induced luciferase expression from the Pai-2 (−2.7 kb) and Pai-2 (−0.8 kb) reporter genes. RAW 264.7 cells were transfected with each reporter gene, with and without pcDNA3-AhR (0 ng, 50 ng, 100 ng) and/or pcDNA3-p65 (1 ng). Values represent the means, normalized to *Renilla* luciferase activity (used as an internal control), ± standard deviations of the results of three independent experiments. The activities shown by the fourth and seventh pairs of bars were used as standards for normalizing the relative activities of the other conditions. (B) AhR WT and AhR KO PEMs were left untreated or were treated with LPS for 1 h. Cytoplasmic (Cyto) and nuclear (Nuc) extracts were immunoblotted with antibodies against AhR, p65, tubulin, and lamin. (C) Co-IP of AhR and p65. Whole-cell extracts from AhR WT PEMs were coimmunoprecipitated with anti-AhR antibody. Co-IPs and Western blotting were performed as described in Materials and Methods. (D) Relative expression levels of Cox-2 mRNA in AhR WT and AhR KO PEMs after 4 h of treatment with or without LPS (10 ng/ml). Bars are as labeled in panel A. Error bars show standard deviations. (E) Top, transcription factor binding sites in the Pai-2 and Cox-2 genes. Bottom, results of ChIP analyses of the Pai-2 and Cox-2 promoters. ChIP analyses were performed using antibodies to p65, AhR, and PolII in LPS-induced AhR WT and AhR KO PEMs. ChIP analyses and real-time PCRs were performed as described in Materials and Methods. Error bars show standard deviations. +, present; −, absent; α, anti; IgG, immunoglobulin G.

volved in Pai-2 expression induced by LPS treatment in the absence of typical AhR ligands (Fig. 4A). The mechanism of AhR's involvement in Pai-2 expression induced by LPS will be investigated in detail. To further address the question of the requirement for the AhR domain in Pai-2 expression, we generated ANA-1 cells stably transfected with AhR ΔC (an activation domain-deficient mutant) and AhR Y9F (the mutant with attenuated DNA binding) (18). Compared with the expression in stable ANA-1 cells transfected with full-length AhR, neither of the cell lines transfected with AhR ΔC or AhR Y9F significantly expressed Pai-2 (Fig. 6B, bars 3 to 6, 9, and 10). These results indicate that both the activation and DNA binding domains of AhR were required for AhR-dependent Pai-2 expression. Co-IP analysis using these AhR mutants showed that the N-terminal region of AhR (AhR ΔC mutant) interacted with p65 (Fig. 6C).

DISCUSSION

AhR was originally found as a transcription factor that was involved in the induction of xenobiotic-metabolizing CYP1A1 by TCDD and other PAHs and has been found to act as a multifunctional regulatory factor in areas ranging from drug metabolism to innate immunity, providing protection against invading xenobiotics. Close investigation of the phenotypes of AhR KO mice revealed that they seem to suffer from morbidity from impaired immunity and easily succumb to bacterial infection. We examined the susceptibility of AhR KO mice to LPS-induced septic shock and found that they were hypersensitive to LPS treatment and had increased secretion of proinflammatory cytokines, such as IL-1β, TNF-α, IL-18, and IFN-γ (Fig. 1A and B). It has been reported that in endotoxic shock, IL-1β and TNF-α are rapidly released and trigger a secondary

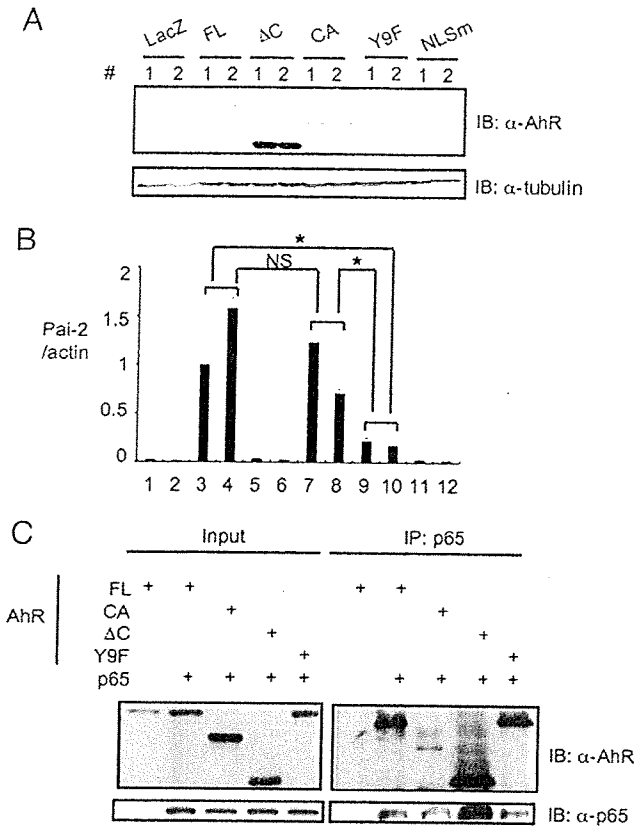

FIG. 6. Nuclear localization, activation, and DNA binding domains of AhR are required for AhR-dependent Pai-2 expression. (A) Immunoblot analysis of full-length AhR or mutants in LacZ or AhR transformant ANA-1 cells. Paired lanes labeled 1 and 2 show results from experiments using two independent transformants. (B) Relative expression levels of Pai-2 mRNA in ANA-1 cells transfected with LacZ or full-length AhR or mutants. Bars show quantification of the results in the 12 lanes in panel A; error bars show standard deviations. *, $P < 0.001$; NS, not significant. (C) Interaction of p65 and AhR mutants. Co-IP of p65 and full-length AhR or mutants expressed in 293T cells, using anti-p65 antibody. AhR FL (full-length) comprises amino acids 1 to 805, AhR ΔC comprises amino acids 1 to 544, and AhR CA comprises amino acids 1 to 276 and 419 to 805; in AhR Y9F, Y9 was mutated to F; and in AhR NLSm 37R, 38H, and 39R were mutated to A, G, and S, respectively. IB, immunoblot; α, anti; +, present.

inflammatory cascade that is dependent on the transcription factor NF-κB (10). Mice with a macrophage-specific conditional deletion of AhR ($AhR^{flox/-}$::LysM Cre) were more susceptible to LPS-induced septic shock than $AhR^{flox/-}$ mice, indicating that the dysfunction of macrophages due to AhR deficiency is one of the major causes of the enhanced susceptibility of AhR KO mice to LPS-induced septic shock (Fig. 2A). Consistent with these observations, isolated AhR KO BMDM secreted much larger amounts of IL-1β and had a slight increase in TNF-α in response to LPS (Fig. 2B). Since IL-1β mRNA levels were not altered between AhR KO and AhR WT BMDM (Fig. 2C), the increased IL-1β secretion is probably not due to the enhanced synthesis but, rather, is likely due to enhanced processing of IL-1β. (16).

We thought that this IL-1β oversecretion by AhR-deficient macrophages might provide clues as to how AhR functions as a physiological immunosuppressor. Microarray analyses to comprehensively investigate the AhR-dependent changes in gene expression that were responsible for increased IL-1β secretion revealed that the levels of expression of Pai-2 and Bcl-2 mRNA were markedly reduced in AhR KO BMDM, which was confirmed by real-time PCR (Fig. 3B). Reconstitution experiments with adenoviruses showed that only Pai-2 expression could significantly suppress IL-1β oversecretion in AhR KO macrophages, while no suppressive effect was observed with Bcl-2 expression (Fig. 3C). It has been reported that there are several pathways for processing IL-1β that lead to its secretion (16). These results indicate that Pai-2 and Bcl-2 are differentially involved in these pathways. Recently, in experiments using ΔIKKβ myeloid mice, Pai-2 has been reported to suppress IL-1β secretion, acting downstream of NF-κB (10). The IL-1β processing that is regulated by the inflammasome involves caspase-1 (16). Consistent with these observations, treatment with caspase inhibitors, Z-YVAD-FMK and Z-VAD-FMK markedly reduced the secretion of IL-1β in AhR KO BMDM (Fig. 3A). It has also been reported that IL-18 processing is regulated by the same mechanism as IL-1β, which is consistent with the marked increase in plasma IL-18 levels ($P < 0.001$) observed in LPS-injected AhR KO mice (Fig. 1B). Stimulation of the inflammasome involving caspase-1 usually requires secondary signals, such as high ATP concentrations. Interestingly, however, the IL-1β oversecretion resulting from AhR deficiency did not seem to require any other stimulation besides LPS, which is in accordance with the report on the IKKβ Δmyeloid mice (10). Further investigation will be required to address the molecular details of Pai-2-regulated IL-1β secretion.

Although it has been reported that Pai-2 mRNA was induced by a typical AhR ligand, TCDD (27), we did not find any obvious XRE sequences (GCGTG) in the 5-kb regions upstream or downstream of the transcription start site of the mouse Pai-2 promoter. However, these promoter regions rendered a reporter gene responsive to LPS (Fig. 5A and E). This sequence search suggested that AhR might not regulate Pai-2 gene expression in the canonical way (i.e., heterodimerized with Arnt) and led us to investigate whether Arnt was involved in LPS-induced Pai-2 regulation. In experiments with Arnt-deficient and Arnt siRNA-expressing macrophages, we demonstrated that AhR enhanced Pai-2 expression in an Arnt-independent manner (Fig. 4D; also see Fig. S1 in the supplemental material). Arnt2 is considered to be another possible alternative (11), but we have previously shown that AhR interacts predominantly with Arnt but not with Arnt2 (27). Therefore, it is highly likely that AhR enhances Pai-2 expression independently of Arnt family proteins (11). It was previously reported that LPS induced Pai-2 expression through activation of NF-κB (21) and that AhR physically interacted with p65 (31) to activate or inhibit gene expression in a context-dependent manner (31). In our reporter gene assay using RAW 264.7 cells, the Pai-2 reporter gene required both NF-κB and AhR for a high level of expression in response to LPS treatment (Fig. 5A). In AhR KO macrophages, LPS treatment induced nuclear translocation of p65 (Fig. 5B), but it was not recruited to the NF-κB-binding site of the Pai-2 gene, which confers LPS inducibility (Fig. 5E), suggesting that AhR is required for recruitment of p65 to this site, which may be a